Structure-Activity Relationships in Human Toll-like Receptor 8-Active 2,3-diamino-furo[2,3-*c*]pyridines

Deepak B. Salunke[†], **Euna Yoo**[†], **Nikunj M. Shukla**[†], **Rajalakshmi Balakrishna**[†], **Subbalakshmi S. Malladi**[†], **Katelyn J. Serafin**[†], **Victor W. Day**[‡], **Xinkun Wang**[§], and **Sunil A. David**[†,*]

[†]Department of Medicinal Chemistry, University of Kansas

[‡]Small-Molecule X-Ray Crystallography Laboratory, University of Kansas

[§]Genomics Facility, University of Kansas

Abstract

In our ongoing search toward identifying novel and synthetically simpler candidate vaccine adjuvants, we hypothesized that the imidazo[1,2-*a*]pyrazines, readily accessible via the Groebke-Blackburn-Bienaymé multicomponent reaction, would possess sufficient structural similarity with TLR7/8-agonistic imidazoquinolines. With pyridoxal as the aldehyde component, furo[2,3-*c*]pyridines, rather than the expected imidazo[1,2-*a*]pyridines were obtained, which were characterized by NMR spectroscopy and crystallography. Several analogues were found to activate TLR8-dependent NF-κB signaling. In a focused library of furo[2,3-*c*]pyridines, a distinct SAR was observed with varying substituents at C2. In human PBMCs, none of the furo[2,3-*c*]pyridines showed any proinflammatory cytokine induction, but upregulated several chemokine ligand genes. In immunization studies in rabbits, the most active compound showed prominent adjuvantic effects. The complete lack of proinflammatory cytokine induction coupled with strong adjuvantic activity of the novel furo[2,3-*c*]pyridines render this hitherto unknown chemotype an attractive class of compounds which are expected to be devoid of local or systemic reactogenicity.

Keywords

TLR8; TLR8 agonists; Vaccine adjuvants; Innate immunity; Furopyridines

Introduction

The innate and adaptive limbs of the immune system are activated in a highly regulated and coordinated manner to initiate host responses to invading pathogens. The innate immune system utilizes germline-encoded pattern recognition receptors (PRRs) to discern pathogen-associated molecular patterns (PAMPs) that are distinct to the pathogen.[1–3] PRRs encompass diverse families of receptors[4] that are secreted into the extracellular environment (such as the collectins,[5] ficolins,[6] pentraxins,[7] alarmins[8]), exist in the cytosol (examples of which include the retinoic acid–inducible gene I–like receptors,[9] and the nucleotide-binding domain and leucine-rich repeat–containing receptors[10]), or are present on membranes.

Important among the transmembrane PRRs include the Toll-like receptors[11] (TLRs) which are either expressed on the plasma membrane or in the endolysosomal compartments.[1] At least 10 functional TLRs are encoded in the human genome, each with an extracellular domain having leucine-rich repeats and a cytosolic domain called the Toll/IL-1 receptor domain.[12] The ligands for these receptors are highly conserved microbial molecules such as lipopolysaccharides (LPS) (recognized by TLR4), lipopeptides (TLR2 in combination with TLR1 or TLR6), flagellin (TLR5), single stranded RNA (TLR7 and TLR8), double stranded RNA (TLR3), CpG motif-containing DNA (recognized by TLR9), and profilin present on uropathogenic bacteria (TLR11).[13] TLR1, -2, -4, -5, and -6 recognize extracellular stimuli, while TLR3, -7, -8 and -9 function within the endolysosomal compartment.[12] The activation of TLRs by their cognate ligands leads to production of inflammatory cytokines, and up-regulation of MHC molecules and co-stimulatory signals in antigen-presenting cells as well as activating natural killer cells (innate immune response), which leads to the priming and amplification of T-, and B-cell effector functions (adaptive immune responses).[14–17]

The discovery of TLRs has not only served to greatly accelerate our understanding of the interplay between the innate and adaptive immune systems, but is also catalyzing novel approaches to vaccine design and development. Several synthetic compounds have been identified as ligands and agonists of the TLRs, leading to detailed SAR studies on these chemotypes. For instance, the S-[2,3-*bis*(palmitoyloxy)-(2*RS*)-propyl]-*R*-cysteinyl-*S*-serine (PAM$_2$CS) lipopeptides[18] and simpler analogues[19,20] activate TLR2. Polyriboinosinic polyribocytidylic acid (poly(I:C)) activates TLR3.[21,22] Synthetic lipid A[23] and various monosaccharide lipid A analogues[24,25] have been reported to activate immune cells by utilizing TLR4. Imidazoquinolines such as imiquimod and resiquimod,[26–28] 2-amino-pyrimidines such as bromopirone,[29,30] guanosine analogues such as loxoribine,[31] and 8-hydroxyadenine derivatives[32,33] are known to activate TLR7 and/or TLR8, while 2-alkylthiazolo[4,5-*c*]quinolin- 4-amine derivatives predominantly activate TLR8 (Figure 1).[34,35]

Small molecule TLR7/8 activators constitute a small set of compounds occupying a very small chemical space, and are represented by substituted imidazo/thiazolo/oxazolo/selenazolo- [4,5-*c*]quinolines **1a-d**, imidazo[4,5-*c*]pyridines **2**, and a few purine and pyrimidine derivatives (Figures 1 and 2). The identification of simpler molecules as TLR7/8 agonists may pave the way for inexpensive vaccine constructs, and we are therefore keenly interested in exploring alternative chemotypes that are synthetically less complex. Unlike TLR2, TLR3, TLR4,[36] and TLR5[37] for which crystal structures are available as complexes with their cognate ligands, a detailed structural characterization of the mode of binding of TLR7 ligands is not yet available to guide scaffold-hopping[38,39] approaches. We speculated that 3,8-diamino-imidazo[1,2-*a*]pyrazines **4** (Figure 2) may bear sufficient structural similarities to the known TLR7/8 ligands (Figures 1 and 2). These molecules are, in principle, readily accessible in two steps (one-pot synthetic process) via the Groebke-Blackburn-Bienaymé multicomponent reaction,[32,33] and we envisaged a rapid elaboration and screening of a library of compounds for TLR7/8 agonistic activities.

We began with the syntheses of small test-libraries of 3,8-diamino-imidazo[1,2- *a*]pyrazines as well as 3-amino-imidazo[1,2-*a*]pyridine/pyrazines (Schemes 1 and 2). Most of these compounds (**5a–5d**, **6–23**) were inactive in NF-κB reporter gene assays specific for human TLR-3, -7, -8, and -9; however compounds **26–29** obtained with pyridoxal as the aldehyde component were found to specifically activate NF-κB signaling in TLR8-transfected HEK293 cells. Detailed spectroscopic analyses confirmed the formation of a hitherto unknown 2,3- diamino-furo[2,3-*c*]pyridine skeleton via a non-canonical pathway, which was unambiguously confirmed by single crystal X-ray analysis. The TLR8-specific agonistic

properties of this novel and unexpected chemotype warranted a systematic SAR, which is presented herein.

Results and Discussion

We have previously described extensive SAR on the 1,2-disubstituted-(1*H*-imidazo[4,5-*c*]quinoline-4-amines) class of compounds[27,28,40,41] (**1a**, Figure 2) as TLR7/8 agonists, and their application in designing self-adjuvanting vaccine constructs.[42] In our ongoing search toward identifying novel and synthetically simpler candidate vaccine adjuvants, we hypothesized that the imidazo[1,2-*a*]pyrazines **4** (Figure 2) would possess sufficient structural similarity with the known small molecule TLR7/8 ligands such as **1**–**3** (Figure 2). These molecules are readily accessible in a one-pot, two-step process using the Groebke-Blackburn-Bienaymé multicomponent reaction as a key step. An acid-catalyzed (HCl in dioxane), microwave-mediated (400W, 110 °C, 10 min) reaction using 2-amino-3-chloropyrazine (amidine component), isocyanocyclohexane (isonitrile component) and benzaldehyde (aldehyde component) resulted, as expected, in 8-chloro-*N*-cyclohexyl-2-phenylimidazo[1,2-*a*]pyrazin-3- amine (Scheme 1). Subsequent microwave-mediated *ipso*-chloro displacement using ammonium hydroxide was unsuccessful, but conventional heating in a sealed tube (110 °C, 16h) furnished the desired N^3-cyclohexyl-2-phenylimidazo[1,2-*a*]pyrazine-3,8-diamine **5a** (Scheme 1) in 30% yield over two steps. Using this one-pot process, a small set of 8-amino-imidazo[1,2-*a*]pyrazines **5b**-**5d** was synthesized by varying the aldehyde and isonitrile components (Scheme 1).

Simultaneously, a diverse test-library comprising of twenty-four compounds was also synthesized (Scheme 2) using two amidines (2-aminopyridine and 2-aminopyrazine), three isonitriles (2-isocyano-2-methylpropane, isocyanocyclohexane, (isocyanomethyl)benzene), and four aldehydes (benzaldehyde, isonicotinaldehyde, salicylaldehyde and pyridoxal). The syntheses of **6**–**23** (Scheme 2) proceeded smoothly. The typical Groebke reaction, carried out at 100 °C for 20 min in CH_3CN, was found to be excessively harsh for reactions using pyridoxal (**24**–**29**), leading to low yields and charring of reaction mixtures. Reactions for this subset of compounds progressed rapidly in 2 min under microwave conditions at 80 °C and 600W power in CH_3CN or MeOH. We noticed that only compounds **24**–**29** (synthesized using pyridoxal) were fluorescent on TLC under long-wave ultraviolet radiation.

The compounds were screened in NF-κB reporter gene assays specific for human TLR-3, -4, -5, -7, -8, and -9. The 3,8-diamino-imidazo[1,2-*a*]pyrazines **5a**-**5d** as well as 3-amino-imidazo[1,2-*a*]pyridine/pyrazine library members **6**–**23** did not display any activity in these assays up to concentrations of 250 μM (Supporting Information). However, compounds **26**–**29** (Scheme 2), obtained with the use of pyridoxal as the aldehyde component, were found to specifically activate NF-κB signaling in human TLR8-transfected HEK293 cells (Table 1, Figure 3), but not human TLR-3, -4, -5, -7, and -9. The NMR spectra of compounds **26**–**29** as well as their fluorescence properties alerted us to the possibility of the formation of a new chemical entity with a heterocyclic system other than the classical imidazo[1,2-*a*]pyridine/pyrazines during the Groebke-Blackburn-Bienaymé multicomponent reaction. In ^{1}H NMR spectra, the aliphatic CH of the cyclohexyl group in compounds **8/9**, **14/15**, and **20/21** (Scheme 2) appeared in the range of 3.0 to 3.1 δ ppm, whereas a pronounced downfield shift of this CH proton (up to 3.85 δ ppm) was observed in compounds **26** and **27**. Similar observations were noted in another set in which the aliphatic benzylic CH_2 in compounds **10/11**, **16/17**, and **22/23** appeared in the range of 4.2 to 4.3 δ ppm, whereas a pronounced downfield shift of this CH_2 (up to 4.76 δ ppm) was observed in compounds **28** and **29**. ^{13}C NMR spectra of compounds **24**–**29** showed an unusual upfield shift of one of the aromatic quaternary carbons in the region (90–96 δ ppm). These observations suggested a different heterocyclic system in **24**–**29**. Initial efforts to crystallize these molecules were

unsuccessful. Pending continuing crystallization efforts, we sought to elucidate the structures of these compounds via alternate routes.

Three possible cyclization products appeared plausible in this acid-catalyzed multicomponent reaction (Panel A in Scheme 3). As mentioned earlier, NMR spectroscopic observations for compounds **24–29** were not congruent with the 4-(3-(cyclohexylamino)imidazo[1,2-*a*]pyridin-2-yl)-5-(hydroxymethyl)-2-methylpyridin-3-ol **32**, the expected product via the canonical Groebke mechanism ('Path A', Panel A in Scheme 3). In order to test whether the phenolic or benzylic hydroxyl groups of pyridoxal may be involved in an alternate pathway of cyclization, we carried out a reaction using a pyridoxal derivative **34** with its phenolic hydroxyl protected with a benzyl group (Scheme 4). This resulted in a product with a spectral signature entirely consistent with the classical Groebke product (5-(benzyloxy)-4- (3-(cyclohexylamino)imidazo[1,2-*a*]pyridin-2-yl)-6-methylpyridin-3-yl)methanol **35**, indirectly also ruling out the possibility of cyclization involving the benzylic hydroxyl group ('Path B', Panel A in Scheme 3). We reasoned that annulation via 'Path C' ought to lead to a furo[2,3- *c*]pyridine skeleton **26**, and that if this were indeed the case, this cyclization could proceed even if the amidine were to be replaced with an aniline. We were gratified that a multicomponent reaction involving aniline, benzyl isonitrile and pyridoxal (Scheme 5) yielded the fluorescent compound **36**, whose ^{1}H and ^{13}C NMR spectra resembled those of compounds **24–29**. Interestingly, **36** was also found to be weakly active (EC_{50} = 1.68 μM) in primary TLR8 screens (Table 1, Figure 3). Our investigations thus far suggested the formation of a hitherto unknown furo[2,3- *c*]pyridine structure, exclusively when pyridoxal was used as the aldehyde component in the Groebke-Blackburn-Bienaymé multicomponent reaction.

Although a definitive elucidation of the reaction mechanism leading to the unexpected furo[2,3- *c*]pyridine was not an immediate goal, understanding plausible mechanisms was of interest, and was probed in some detail. Formation of the pyrano[3,4-*c*]pyridine **33** via nucleophilic attack of the benzylic hydroxyl group, and its subsequent rearrangement to the furo[2,3-*c*]pyridine **26** (Path D, Panel A in Scheme 3) appeared improbable. Salicylaldehyde, which lacks the bulky hydroxymethylene group, yielded the classical imidazo[1,2-*a*]pyridine **20** (confirmed by single crystal X-ray analysis, see below), rather than the benzofuran derivative **B.3** (Panel B in Scheme 3). We reasoned, therefore, that the benzylic hydroxyl in the transition state **31** could assist cyclization via Path C (Panel A in Scheme 3) due to steric reasons, apposing the phenolic hydroxyl with the electrophilic carbon. In addition to the direct formation of the furo[2,3- *c*]pyridine **26** via path C, a plausible alternate mechanism for this unusual cyclization route, involving the pyridine ring system is proposed in Scheme 3 (Panel C).

After many unsuccessful attempts, a hydrochloride salt of compound **28** was crystallized as multiply-twinned bundles in acetonitrile. A multi-domain specimen of **28** was cut from one bundle which gave a set of diffracted intensities, permitting a crystal structure solution (noncentrosymmetric, triclinic P1-C1 space group with eight crystallographically-independent molecules in the asymmetric unit), but not a satisfactory refinement (Figure 4). The structure of **28** unambiguously confirmed the furo[2,3-*c*]pyridine chemotype. The structure of compound **20** (obtained with salicylaldehyde, which also possesses a phenolic OH; Scheme 2) was also elucidated, which established the formation of a classic Groebke product 2-(3- (cyclohexylamino)imidazo[1,2-*a*]pyridin-2-yl)phenol (Figure 4). These observations clearly emphasize the significance of the additional substituents of pyridoxal, directing the unique cyclization route leading to the furo[2,3-*c*]pyridine scaffold.

Thus, our initial attempts toward the synthesis of twenty-four membered imidazo[1,2-*a*]pyrazine/pyridine test-library unexpectedly resulted in the formation of densely substituted

furo[2,3-*c*]pyridines **24–29**. Pyridoxal was found to be an indispensable component for this cyclization reaction. Four of the six compounds obtained (**26–29**, Scheme 2) were found to be active in our primary screens using TLR8-transfected HEK293 cells, while compounds **24** and **25**, synthesized using 2-isocyano-2-methylpropane as one of the components, were found to be inactive, warranting detailed structure based activity relationship investigations for this new chemotype.

Among the active compounds **26–29**, we observed that compounds **26** and **28** (derived from 2-aminopyridine), were more active than **27** and **29** (from 2-aminopyrazine; Table 1, Figure 3). We therefore selected 2-aminopyridine and pyridoxal as the invariant components and varied the isonitrile component. We explored thirteen different isonitriles (Scheme 6), including linear aliphatic (as in **37a** and **37b**), branched aliphatic (**37c-37e**), linear aliphatic with silyl (**37f**), heteroaromatic ring (**37g**), ester (**37h**, **37i**), and phosphate ester (**37j**) termini, as well as aromatic substituents (**37k-37m**). Maximal activity was observed in **37b**, with a pentylene substituent on the C2 amine (Scheme 6, Figure 3). Diminishing the chain length by one methylene unit (**37a**) decreased activity, and potency was further attenuated in compounds with alpha-branched substituents (**37d**). Compound **37n**, with a free NH_2 at C2, obtained by *N*-dealkylation of the *tert*-octylamine group[43] of **37e** with trifluoroacetic acid, as well as compounds with aromatic substituents (**37k-37m**) were devoid of TLR8-stimulatory activity (Table 1). Thus, a distinct dependence of the nature of the C2 amino substituent on the activity profiles was observed in the furo[2,3-*c*]pyridines, with the C2-*N*-pentyl (**37b**) and C2-*N*-(trimethylsilyl)methyl analogues (**37f**) displaying dominant TLR8 agonism.

As mentioned earlier, our earlier efforts at unambiguously confirming the structure of **28** did not allow for satisfactory crystal structure refinement because of the intrinsic properties of the crystal space group. Having synthesized thirteen additional furo[2,3-*c*]pyridines (**37a-37m**) for purposes of delineating SAR, a parallel crystallization of these compounds was attempted using various solvents. Suitable crystals of compound **37e** were obtained as pale yellow crystals by slow evaporation of a super-saturated solution of **37e** in CH_3CN/ CH_3OH mixtures at room temperature. A single-domain specimen was selected and the X-ray diffraction data was collected. The ORTEP diagram of **37e** is shown in Figure 5, confirming the non-Groebke furo[2,3-*c*]pyridine.

Previous mention was made that **36** (Scheme 5) was found to be weakly active (EC_{50} = 1.68 µM, Table 1, Figure 3B) relative to the lead compound **28**, suggesting that the 2-aminopyridine core could be substituted by anilines in this multicomponent reaction. Having optimized the C2 group as pentylamine (derived from 1-isocyanopentane, Scheme 6), three more furo[2,3-*c*]pyridines were synthesized using aniline **38a**, 3-fluoroaniline **38b** and 3-nitroaniline **38c** in combination with 1-isocyanopentane and pyridoxal (Scheme 7). The C2 *N*-pentyl analogue **38a** was found to be more active than the C2 *N*-benzyl analogue **36** (Figure 3A and 3B, Table 1). The nitro derivative **38c** was found to be as potent as the parent compound **38a**, whereas substantial gain in TLR8 activity was noticed for the fluoro-substituted compound **38b** in TLR8-specific functional assays. However, these compounds exhibited a poorer dose-response profile (lower area-under the-curve, Figure 3). It is pertinent to note that no stable product could be obtained by the replacement of 2-aminopyridine with aliphatic amines.

Several TLRs are thought to signal via ligand-induced dimerization,[44] as evident in the crystal structures of TLR2[36,45] and TLR3.[21] It is not yet understood, however, how TLR7 and TLR8, whose endogenous ligands are single-stranded viral RNA (ssRNA), recognize and transduce signals upon engagement by small, non-polymeric molecules such as the imidazoquinolines[26,46] and the oxoadenines.[47,48] In order to probe possible mechanisms of

ligand recognition by TLR8, the dimeric compound **39** was synthesized using 1,6-diisocyanohexane (Scheme 8); the activity of this analogue was comparable in its TLR8-agonistic potency to the most active compounds, **28**, **37a**, **37b** and **37f** (Table 1).

We examined the cytokine-inducing properties[49,50] of a subset of compounds that were maximally active (**28**, **37a**, **37b** and **37f**), all of which showed robust dose-response profiles in primary TLR8-agonistic screens (Figure 3). We used 2-propylthiazolo[4,5-*c*]quinolin-4-amine **40** (CL075) as a reference TLR8 agonist,[34,35] which exhibited an EC_{50} of 1.32 µM (Figure 3). In human PBMCs, only the reference thiazoloquinoline **40**, but none of the furo[2,3-*c*]pyridines showed any proinflammatory cytokine induction (Figure 6). We do not yet know if the dissociation between TLR8-specific NF-κB induction on the one hand, and lack of cytokine induction on the other is ascribable to a non-myeloid differentiation primary response gene 88 (MyD88)-independent mechanism.[51,52] However, mindful of recent observations that proinflammatory activity is not an absolute prerequisite for adjuvantic properties,[53] and because we had previously observed potent NF-κB transactivation in a *bis*-quinoline, 7-chloro-*N*-(4-(7-chloroquinolin-4-ylamino)butyl) quinolin-4-amine **41** (RE-660)[54] unaccompanied by any proinflammatory cytokine induction, we decided to examine two representative compounds (**37b** and **37f**) in transcriptomal profiling experiments. Consistent with the cytokine assays, there were no transcriptional signatures of inflammation; however, both compounds upregulated several chemokine ligand (both CXCL and CCL) genes (Supporting Information). Although entirely bereft of any proinflammatory activity, the *bis*-quinoline compound **41** was found to be a potent adjuvant which appears to be related to its functional agonism at CCR1.[54] Given some similarities in activity profiles between the furo[2,3-*c*]pyridines and **41**, we decided to evaluate and compare the adjuvantic activity of **37b** alongside the reference compounds, **40** and **41**. Rabbits were immunized using bovine α-lactalbumin as a model subunit antigen.[42] Anti-α-lactalbumin IgG titers in immune sera clearly show an adjuvantic effect of **37b**, with a rise-in-titer values of >1000, comparable to the adjuvantic activities of the reference compounds, **40** and **41** (Figure 7). The complete lack of proinflammatory cytokine induction coupled with strong adjuvantic activity of the novel furo[2,3-*c*]pyridines render this hitherto unknown chemotype an exceedingly attractive class of compounds which are expected to be devoid of local or systemic reactogenicity. Further structure-activity studies on the furopyridines and related chemotypes are currently in progress.

Experimental Section

Chemistry

All of the solvents and reagents used were obtained commercially and used as such unless noted otherwise. Moisture- or air-sensitive reactions were conducted under nitrogen atmosphere in oven-dried (120 °C) glass apparatus. The solvents were removed under reduced pressure using standard rotary evaporators. Flash column chromatography was carried out using RediSep Rf 'Gold' high performance silica columns on CombiFlash Rf instrument unless otherwise mentioned, while thin-layer chromatography was carried out on silica gel (200 µm) CCM pre-coated aluminum sheets. The purity of all final compounds was confirmed to be greater than 95% by HPLC-MS using a Zorbax Eclipse Plus 4.6 mm x 150 mm, 5 µm analytical reverse phase C18 column with either H_2O-isopropanol or H_2O-CH_3CN gradients, a diode-array detector operating in 190–500 nm range (2 nm bandpass), and an Agilent ESI-TOF mass spectrometer (integration on total ion intensity counts, with a mass accuracy of 10 ppm) operating in the positive ion acquisition mode.

General procedure for the syntheses of compounds 5a-5f

Synthesis of compound 5a: N^3-cyclohexyl-2-phenylimidazo[1,2-a]pyrazine-3,8-diamine

To a solution of 2-amino-3-chloropyrazine (64 mg, 0.50 mmol) in anhydrous acetonitrile (1 mL), were added benzaldehyde (60μL, 0.60 mmol), 4N HCl/dioxane (10μL) and cyclohexylisonitrile (74 μL, 0.60 mmol). The reaction mixture was then heated under microwave conditions (400 W, 110 °C) in a sealed vial for 20 min. The reaction mixture was cooled to room temperature; ammonium hydroxide (NH_3 content 28–30%, 0.5 mL) was added and further heated at 110 °C in a sealed vial for overnight. After cooling the reaction mixture to room temperature, the solvents were removed and the residue was purified using column chromatography to obtain the compound **5a** (47 mg, 30%). ^{1}H NMR (500 MHz, MeOD) δ 8.02 (dd, J = 8.2, 1.3 Hz, 2H), 7.64 (d, J = 4.8 Hz, 1H), 7.46 (dd, J= 10.9, 4.6 Hz, 2H), 7.39 – 7.28 (m, 1H), 7.21 (d, J = 4.8 Hz, 1H), 2.96 – 2.83 (m, 1H), 1.76 (d, J = 11.6 Hz, 2H), 1.71 – 1.62 (m, 2H), 1.57-1.51 (m, 1H), 1.31 – 1.19 (m, 2H), 1.19 – 1.03 (m, 3H).^{13}C NMR (126 MHz, MeOD) δ 151.14, 136.46, 135.17, 129.95, 129.55, 129.44, 128.67, 128.24, 128.11, 109.02, 57.87, 35.05, 26.86, 25.99. MS (ESI) calcd for $C_{18}H_{21}N_5$, m/z 307.1797, found 308.1923 $(M+H)^+$.

Compounds **5b**-**5d** were synthesized similarly as compound **5a**.

5b: 2-([1,1′-biphenyl]-4-yl)-N^3-cyclohexylimidazo[1,2-a]pyrazine-3,8-diamine

(44 mg, 23%) ^{1}H NMR (500 MHz, MeOD) δ 8.13 (d, J = 8.2 Hz, 2H), 7.72 (d, J = 8.3 Hz, 2H), 7.71 – 7.67 (m, 2H), 7.64 (d, J = 4.8 Hz, 1H), 7.45 (t, J = 7.7 Hz, 2H), 7.38 – 7.31 (m, 1H), 7.22 (d, J = 4.8 Hz, 1H), 3.02 – 2.84 (m, 1H), 1.80 (d, J = 12.2 Hz, 2H), 1.69 (dd, J = 8.2, 5.3 Hz, 2H), 1.55 (s, 1H), 1.35 – 1.23 (m, 2H), 1.24 – 1.01 (m, 3H). ^{13}C NMR (126 MHz, MeOD) δ 151.16, 141.92, 141.53, 136.10, 134.18, 130.07, 129.93, 129.56, 128.57, 128.45, 128.13, 128.02, 127.86, 109.03, 57.99, 35.12, 26.88, 26.03. MS (ESI) calcd for $C_{24}H_{25}N_5$, m/z 383.2110, found 384.2382 $(M+H)^+$.

5c: N^3-benzyl-2-butylimidazo[1,2-a]pyrazine-3,8-diamine

(10 mg, 7%) ^{1}H NMR (500 MHz, MeOD) δ 7.44 (d, J = 4.8 Hz, 1H), 7.29 – 7.17 (m, 5H), 7.12 (d, J = 4.8 Hz, 1H), 4.13 (s, 2H), 2.51 – 2.42 (m, 2H), 1.54 – 1.42 (m, 2H), 1.31 (dq, J = 14.8, 7.4 Hz, 2H), 0.91 (t, J = 7.4 Hz, 3H). ^{13}C NMR (126 MHz, MeOD) δ 150.52, 141.10, 138.98, 130.14, 129.57, 129.49, 128.81, 128.40, 127.74, 108.93, 53.28, 32.76, 27.26, 23.73, 14.26. MS (ESI) calcd for $C_{17}H_{21}N_5$, m/z 295.1797, found 296.1952 $(M+H)^+$.

5d: 2-butyl-N^3-(4-methoxyphenyl)imidazo[1,2-a]pyrazine-3,8-diamine

(36 mg, 23%) ^{1}H NMR (500 MHz, MeOD) δ 7.26 (d, J = 4.7 Hz, 1H), 7.16 (d, J = 4.7 Hz, 1H), 6.80 – 6.69 (m, 2H), 6.49 – 6.38 (m, 2H), 3.70 (s, 3H), 2.67 (t, J = 7.6 Hz, 2H), 1.73 – 1.62 (m, 2H), 1.41 – 1.23 (m, 2H), 0.88 (t, J = 7.4 Hz, 3H). ^{13}C NMR (126 MHz, MeOD) δ 154.65, 150.75, 142.09, 140.98, 129.90, 128.28, 124.98, 115.97, 115.50, 109.10, 56.07, 32.40, 27.41, 23.46, 14.15. MS (ESI) calcd for $C_{17}H_{21}N_5O$, m/z 311.1746, found 312.1905 $(M +H)^+$.

General procedure for the syntheses of compounds 6–29

Synthesis of compound 6: N-(tert-butyl)-2-phenylimidazo[1,2-a]pyridin-3-amine

To a solution of 2-aminopyridine (24 mg, 0.25 mmol) in anhydrous acetonitrile, were added benzaldehyde (28 μL, 0.28 mmol), 4N HCl/dioxane (5 μL) and tert-butyl isonitrile (27 μL, 0.24 mmol). The reaction mixture was then heated under microwave conditions (400 W, 110 °C) in a sealed vial for 20 min. After cooling the reaction mixture to room temperature, the solvents were removed and the residue was purified using column chromatography to obtain compound **6** (44 mg, 70%). ^{1}H NMR (400 MHz, CDCl_3) δ 8.23 (dt, J = 6.9, 1.2 Hz, 1H), 7.90 (dt, J = 8.1, 1.6 Hz, 2H), 7.55 (dt, J = 9.0, 1.0 Hz, 1H), 7.43 (t,

J = 7.6 Hz, 2H), 7.31 (t, J = 7.4 Hz, 1H), 7.13 (ddd, J = 9.0, 6.6, 1.3 Hz, 1H), 6.77 (td, J = 6.8, 1.1 Hz, 1H), 3.12 (s, 1H), 1.04 (s, 9H). ^{13}C NMR (101 MHz, CDCl$_3$) δ 142.15, 135.42, 135.40, 128.43, 128.32, 127.52, 124.17, 123.64, 117.48, 111.46, 101.91, 56.59, 30.43. MS (ESI) calcd for C$_{17}$H$_{19}$N$_3$, *m/z* 265.1579, found 266.1664 (M+H)$^+$.

Compounds **7**–**29** were synthesized similarly as compound **6**.

7: *N*-(*tert*-butyl)-2-phenylimidazo[1,2-*a*]pyrazin-3-amine—(47 mg, 74%) ^{1}H NMR (400 MHz, CDCl$_3$) δ 9.00 (d, J = 1.4 Hz, 1H), 8.14 (dd, J = 4.6, 1.5 Hz, 1H), 7.91 (dd, J = 8.3, 1.3 Hz, 2H), 7.86 (d, J = 4.6 Hz, 1H), 7.46 (t, J = 7.5 Hz, 2H), 7.37 (t, J = 7.4 Hz, 1H), 3.19 (s, 1H), 1.05 (s, 9H). ^{13}C NMR (101 MHz, CDCl$_3$) δ 143.54, 142.40, 137.43, 134.38, 129.04, 128.66, 128.38, 128.33, 125.17, 116.49, 57.11, 30.45. MS (ESI) calcd for C$_{16}$H$_{18}$N$_4$, *m/z* 266.1531, found 267.1588 (M+H)$^+$.

8: *N*-cyclohexyl-2-phenylimidazo[1,2-*a*]pyridin-3-amine—(64 mg, 86%) ^{1}H NMR (500 MHz, CDCl$_3$) δ 8.16 (d, J = 6.8 Hz, 1H), 8.05 (dd, J = 8.3, 1.2 Hz, 2H), 7.62 (d, J = 9.0 Hz, 1H), 7.45 (t, J = 7.8 Hz, 2H), 7.32 (t, J = 7.4 Hz, 1H), 7.17 (ddd, J = 8.9, 6.7, 1.2 Hz, 1H), 6.82 (td, J = 6.8, 0.9 Hz, 1H), 3.32 (s, 1H), 3.07 – 2.85 (m, 1H), 1.81 (d, J = 13.1 Hz, 2H), 1.68 (dd, J = 9.1, 3.6 Hz, 2H), 1.60 – 1.54 (m, 1H), 1.28 – 1.12 (m, 5H). ^{13}C NMR (126 MHz, CDCl$_3$) δ 141.02, 135.43, 133.45, 128.74, 127.74, 127.20, 125.17, 125.04, 123.07, 116.94, 112.30, 57.02, 34.27, 25.81, 24.94. MS (ESI) calcd for C$_{19}$H$_{21}$N$_3$, *m/z* 291.1735, found 292.1832 (M+H)$^+$.

9: *N*-cyclohexyl-2-phenylimidazo[1,2-*a*]pyrazin-3-amine—(25 mg, 36%) ^{1}H NMR (500 MHz, CDCl$_3$) δ 8.99 (d, J = 1.4 Hz, 1H), 8.01 (ddd, J = 4.6, 3.2, 1.8 Hz, 3H), 7.85 (d, J = 4.6 Hz, 1H), 7.48 (t, J = 7.7 Hz, 2H), 7.38 (t, J = 7.4 Hz, 1H), 3.26 (s, 1H), 3.00 (m, 1H), 2.22 (s, 1H), 1.82 (dd, J = 6.6, 5.4 Hz, 2H), 1.70 (dd, J = 9.3, 3.3 Hz, 2H), 1.62 – 1.55 (m, 1H), 1.34 – 1.07 (m, 5H). ^{13}C NMR (126 MHz, CDCl$_3$) δ 143.37, 139.08, 136.82, 133.62, 129.01, 128.90, 128.30, 127.42, 126.70, 115.73, 57.02, 34.41, 25.69, 24.91. MS (ESI) calcd for C$_{18}$H$_{20}$N$_4$, *m/z* 292.1688, found 293.1775 (M+H)$^+$.

10: *N*-benzyl-2-phenylimidazo[1,2-*a*]pyridin-3-amine—(62 mg, 86%) ^{1}H NMR (500 MHz, CDCl$_3$) δ 7.98 (ddt, J = 3.7, 3.0, 1.6 Hz, 3H), 7.57 (dt, J = 9.0, 1.0 Hz, 1H), 7.45 (t, J = 7.7 Hz, 2H), 7.39 – 7.26 (m, 6H), 7.13 (ddd, J = 9.0, 6.7, 1.3 Hz, 1H), 6.74 (td, J = 6.8, 1.1 Hz, 1H), 4.20 (d, J = 6.1 Hz, 2H), 3.52 (t, J = 6.0 Hz, 1H), 2.45 (s, 1H). ^{13}C NMR (126 MHz, CDCl$_3$) δ 141.57, 139.06, 136.04, 134.13, 128.84, 128.30, 127.82, 127.65, 127.16, 125.77, 124.32, 122.50, 117.52, 111.94, 52.57. MS (ESI) calcd for C$_{20}$H$_{17}$N$_3$, *m/z* 299.1422, found 300.1490 (M+H)$^+$.

11: *N*-benzyl-2-phenylimidazo[1,2-*a*]pyrazin-3-amine—(45 mg, 62%) ^{1}H NMR (500 MHz, CDCl$_3$) δ 8.98 (d, J = 1.3 Hz, 1H), 7.94 (dt, J = 8.1, 1.6 Hz, 2H), 7.82 (dd, J = 4.6, 1.4 Hz, 1H), 7.77 (d, J = 4.6 Hz, 1H), 7.47 (t, J = 7.6 Hz, 2H), 7.39 (t, J = 7.4 Hz, 1H), 7.34 – 7.27 (m, 5H), 4.23 (d, J = 2.4 Hz, 2H), 3.66 (s, 1H), 2.20 (s, 1H). ^{13}C NMR (126 MHz, CDCl$_3$) δ 143.46, 138.76, 138.56, 136.79, 133.34, 129.06, 129.03, 128.99, 128.46, 128.24, 128.08, 127.42, 127.18, 115.38, 52.39. MS (ESI) calcd for C$_{19}$H$_{16}$N$_4$, *m/z* 300.1375, found 301.1494 (M+H)$^+$.

12: *N*-(*tert*-butyl)-2-(pyridin-4-yl)imidazo[1,2-*a*]pyridin-3-amine—(50 mg, 78%) ^{1}H NMR (500 MHz, CDCl$_3$) δ 8.65 (d, J = 5.9 Hz, 2H), 8.20 (dt, J = 6.9, 1.0 Hz, 1H), 7.96 (dd, J = 4.7, 1.4 Hz, 2H), 7.56 (d, J = 9.1 Hz, 1H), 7.18 (ddd, J = 9.0, 6.6, 1.2 Hz, 1H), 6.81 (td, J = 6.8, 1.0 Hz, 1H), 3.07 (s, 1H), 1.10 (s, 9H). ^{13}C NMR (126 MHz, CDCl$_3$) δ 149.69,

142.82, 142.39, 136.46, 124.86, 124.77, 123.38, 122.17, 117.68, 111.82, 56.78, 30.38. MS (ESI) calcd for $C_{16}H_{18}N_4$, *m/z* 266.1531, found 267.1747 (M+H)$^+$.

13: *N*-(*tert*-butyl)-2-(pyridin-4-yl)imidazo[1,2-*a*]pyrazin-3-amine—(49 mg, 76%) ^{1}H NMR (500 MHz, CDCl$_3$) δ 9.02 (d, *J* = 1.4 Hz, 1H), 8.69 (dd, *J* = 4.5, 1.6 Hz, 2H), 8.11 (dd, *J* = 4.7, 1.5 Hz, 1H), 7.94 (dd, *J* = 4.5, 1.6 Hz, 2H), 7.88 (d, *J* = 4.7 Hz, 1H), 3.12 (s, 1H), 1.10 (s, 9H). ^{13}C NMR (126 MHz, CDCl$_3$) δ 150.22, 144.25, 141.96, 139.25, 137.72, 129.39, 126.24, 122.42, 116.42, 57.46, 30.61. MS (ESI) calcd for $C_{15}H_{17}N_5$, *m/z* 267.1484, found 268.1705 (M+H)$^+$.

14: *N*-cyclohexyl-2-(pyridin-4-yl)imidazo[1,2-a]pyridin-3-amine—(69 mg, 98%) ^{1}H NMR (500 MHz, CDCl$_3$) δ 8.64 (dd, *J* = 4.6, 1.6 Hz, 2H), 8.07 (dt, *J* = 6.9, 1.2 Hz, 1H), 8.00 (dd, *J* = 4.6, 1.6 Hz, 2H), 7.54 (dt, *J* = 9.1, 1.0 Hz, 1H), 7.17 (ddd, *J* = 9.1, 6.6, 1.3 Hz, 1H), 6.81 (td, *J* = 6.8, 1.1 Hz, 1H), 3.11 (d, *J* = 3.9 Hz, 1H), 2.98 (td, *J* = 10.3, 4.1 Hz, 1H), 1.83 (d, *J* = 10.8 Hz, 2H), 1.71 (dd, *J* = 9.4, 3.3 Hz, 2H), 1.59 (dd, *J* = 7.3, 1.4 Hz, 1H), 1.32 – 1.09 (m, 5H). ^{13}C NMR (126 MHz, CDCl$_3$) δ 150.03, 142.26, 142.11, 133.78, 126.92, 124.92, 122.87, 121.21, 117.99, 112.31, 57.26, 34.42, 25.75, 24.97. MS (ESI) calcd for $C_{18}H_{20}N_4$, *m/z* 292.1688, found 293.1854 (M+H)$^+$.

15: *N*-cyclohexyl-2-(pyridin-4-yl)imidazo[1,2-*a*]pyrazin-3-amine—(56 mg, 80%) ^{1}H NMR (500 MHz, CDCl$_3$) δ 9.01 (d, *J* = 1.5 Hz, 1H), 8.70 (dd, *J* = 4.5, 1.6 Hz, 2H), 8.03 – 7.93 (m, 3H), 7.88 (d, *J* = 4.6 Hz, 1H), 3.21 (d, *J* = 5.9 Hz, 1H), 3.06 – 2.97 (m, 1H), 1.84 (d, *J* = 10.5 Hz, 2H), 1.72 (dd, *J* = 9.7, 2.6 Hz, 2H), 1.63 – 1.58 (m, 1H), 1.31 – 1.14 (m, 5H). ^{13}C NMR (126 MHz, CDCl$_3$) δ 150.42, 144.32, 141.25, 137.17, 135.99, 129.45, 128.03, 121.37, 115.69, 57.35, 34.55, 25.62, 24.93.MS (ESI) calcd for $C_{17}H_{19}N_5$, *m/z* 293.1640, found 294.1894 (M+H)$^+$.

16: *N*-benzyl-2-(pyridin-4-yl)imidazo[1,2-a]pyridin-3-amine—(54 mg, 75%) ^{1}H NMR (500 MHz, CDCl$_3$) δ 8.62 (dd, *J* = 4.6, 1.6 Hz, 2H), 7.94 (dt, *J* = 6.9, 1.1 Hz, 1H), 7.90 (dd, *J* = 4.6, 1.6 Hz, 2H), 7.55 (dt, *J* = 9.1, 1.0 Hz, 1H), 7.34 – 7.27 (m, 5H), 7.17 (ddd, *J* = 9.1, 6.6, 1.3 Hz, 1H), 6.76 (td, *J* = 6.8, 1.1 Hz, 1H), 4.22 (d, *J* = 6.1 Hz, 2H), 3.52 (t, *J* = 6.1 Hz, 1H). ^{13}C NMR (126 MHz, CDCl$_3$) δ 150.12, 142.11, 141.94, 138.64, 133.41, 128.98, 128.31, 128.06, 127.46, 125.05, 122.50, 121.13, 118.06, 112.42, 52.64. MS (ESI) calcd for $C_{19}H_{16}N_4$, *m/z* 300.1375, found 301.1599 (M+H)$^+$.

17: *N*-benzyl-2-(pyridin-4-yl)imidazo[1,2-*a*]pyrazin-3-amine—(47 mg, 65%) ^{1}H NMR (500 MHz, CDCl$_3$) δ 9.01 (d, *J* = 1.4 Hz, 1H), 8.67 (dd, *J* = 4.5, 1.6 Hz, 2H), 7.87 (dd, *J* = 4.5, 1.6 Hz, 2H), 7.78 (dt, *J* = 4.6, 3.0 Hz, 2H), 7.30 (dd, *J* = 5.1, 1.9 Hz, 3H), 7.24 (dd, *J* = 6.9, 2.6 Hz, 2H), 4.25 (d, *J* = 6.2 Hz, 2H), 3.66 (t, *J* = 6.2 Hz, 1H). ^{13}C NMR (126 MHz, CDCl$_3$) δ 150.46, 144.33, 140.94, 138.23, 137.12, 135.70, 129.45, 129.14, 128.45, 128.32, 128.25, 121.34, 115.35, 52.59. MS (ESI) calcd for $C_{18}H_{15}N_5$, *m/z* 301.1327, found 302.1474 (M+H)$^+$.

18: 2-(3-(*tert*-butylamino)imidazo[1,2-*a*]pyridin-2-yl)phenol—(20 mg, 30%) ^{1}H NMR (500 MHz, CDCl$_3$) δ 12.47 (bs, 1H), 8.19 (d, *J* = 6.9 Hz, 1H), 8.12 (dd, *J* = 7.8, 1.6 Hz, 1H), 7.51 (d, *J* = 9.0 Hz, 1H), 7.24 – 7.17 (m, 2H), 7.07 – 6.97 (m, 1H), 6.95 – 6.87 (m, 1H), 6.83 (td, *J* = 6.8, 0.9 Hz, 1H), 3.16 (bs, 1H), 1.16 (s, 9H). ^{13}C NMR (126 MHz, CDCl$_3$) δ 157.07, 148.51, 140.76, 138.42, 134.51, 131.35, 129.43, 128.13, 124.82, 123.01, 118.69, 117.76, 116.96, 112.09, 109.94, 57.22, 30.50. MS (ESI) calcd for $C_{17}H_{19}N_3O$, *m/z* 281.1528, found 282.1770 (M+H)$^+$.

19: 2-(3-(*tert*-butylamino)imidazo[1,2-*a*]pyrazin-2-yl)phenol—(40 mg, 59%) ^{1}H NMR (500 MHz, CDCl$_3$) δ 11.87 (s, 1H), 8.98 (d, *J* = 1.4 Hz, 1H), 8.16 – 8.08 (m, 2H), 7.92 (d, *J* = 4.6 Hz, 1H), 7.31 – 7.24 (m, 1H), 7.05 (dd, *J* = 8.2, 1.0 Hz, 1H), 6.93 (td, *J* = 7.9, 1.2 Hz, 1H), 3.22 (bs, 1H), 1.17 (s, 9H). ^{13}C NMR (126 MHz, CDCl$_3$) δ 157.08, 142.79, 140.85, 135.93, 130.39, 129.72, 128.31, 123.47, 119.03, 118.04, 117.65, 115.85, 57.73, 30.54. MS (ESI) calcd for C$_{16}$H$_{18}$N$_4$O, *m/z* 282.1481, found 283.1690 (M+H)[+].

20: 2-(3-(cyclohexylamino)imidazo[1,2-a]pyridin-2-yl)phenol—(30 mg, 41%) ^{1}H NMR (500 MHz, CDCl$_3$) δ 13.16 (s, 1H), 8.17 (d, *J* = 6.8 Hz, 1H), 8.04 (dd, *J* = 7.8, 1.3 Hz, 1H), 7.50 (dt, *J* = 9.0, 0.9 Hz, 1H), 7.25 – 7.17 (m, 2H), 7.04 (dd, *J* = 8.2, 1.1 Hz, 1H), 6.95 – 6.89 (m, 1H), 6.87 (td, *J* = 6.8, 1.0 Hz, 1H), 3.17 – 2.99 (m, 2H), 1.83 (d, *J* = 12.5 Hz, 2H), 1.72 (dd, *J* = 9.5, 3.1 Hz, 2H), 1.64 – 1.57 (m, 1H), 1.32 (dd, *J* = 22.7, 11.7 Hz, 2H), 1.26 – 1.13 (m, 3H). ^{13}C NMR (126 MHz, CDCl$_3$) δ 157.67, 139.51, 136.00, 129.25, 126.41, 124.88, 123.55, 122.62, 118.82, 117.84, 117.40, 116.64, 112.46, 57.08, 34.19, 25.83, 24.96. MS (ESI) calcd for C$_{19}$H$_{21}$N$_3$O, *m/z* 307.1685, found 308.1995 (M+H)[+].

21: 2-(3-(cyclohexylamino)imidazo[1,2-*a*]pyrazin-2-yl)phenol—(54 mg, 73%) ^{1}H NMR (500 MHz, CDCl$_3$) δ 12.52 (bs, 1H), 8.96 (d, *J* = 1.4 Hz, 1H), 8.05 (ddd, *J* = 9.5, 6.2, 1.5 Hz, 2H), 7.94 (d, *J* = 4.6 Hz, 1H), 7.30 – 7.26 (m, 1H), 7.07 (dd, *J* = 8.2, 1.1 Hz, 1H), 6.94 (td, *J* = 8.0, 1.2 Hz, 1H), 3.31 – 2.99 (m, 2H), 1.83 (d, *J* = 12.3 Hz, 2H), 1.77 – 1.70 (m, 2H), 1.62 (dd, *J* = 7.5, 2.3 Hz, 1H), 1.33 (dd, *J* = 21.3, 10.5 Hz, 2H), 1.27 – 1.15 (m, 3H). ^{13}C NMR (126 MHz, CDCl$_3$) δ 157.70, 142.41, 138.53, 134.72, 130.19, 129.97, 126.50, 125.10, 119.13, 118.09, 116.60, 115.35, 57.17, 34.34, 25.69, 24.92. MS (ESI) calcd for C$_{18}$H$_{20}$N$_4$O, *m/z* 308.1637, found 309.1856 (M+H)[+].

22: 2-(3-(benzylamino)imidazo[1,2-*a*]pyridin-2-yl)phenol—(10 mg, 13%) ^{1}H NMR (500 MHz, CDCl$_3$) δ 13.02 (s, 1H), 8.06 – 7.95 (m, 2H), 7.51 (d, *J* = 9.0 Hz, 1H), 7.42 – 7.29 (m, 5H), 7.25 – 7.17 (m, 2H), 7.06 (dd, *J* = 8.2, 1.0 Hz, 1H), 6.95 – 6.89 (m, 1H), 6.80 (td, *J* = 6.8, 0.9 Hz, 1H), 4.24 (bs, 2H), 3.41 (s, 1H).^{13}C NMR (126 MHz, CDCl$_3$) δ 157.75, 139.49, 138.91, 135.58, 129.38, 128.96, 128.43, 127.97, 125.95, 124.95, 124.41, 122.19, 119.04, 117.88, 117.21, 116.74, 112.51, 52.43. MS (ESI) calcd for C$_{20}$H$_{17}$N$_3$O, *m/z* 315.1372, found 316.1611 (M+H)[+].

23: 2-(3-(benzylamino)imidazo[1,2-*a*]pyrazin-2-yl)phenol—(43 mg, 57%) ^{1}H NMR (500 MHz, CDCl$_3$) δ 12.40 (bs, 1H), 8.95 (d, *J* = 1.4 Hz, 1H), 8.02 (dd, *J* = 7.9, 1.6 Hz, 1H), 7.82 (d, *J* = 4.6 Hz, 1H), 7.78 (dd, *J* = 4.6, 1.4 Hz, 1H), 7.37 – 7.27 (m, 6H), 7.09 (dd, *J* = 8.3, 1.2 Hz, 1H), 6.94 (ddd, *J* = 7.9, 7.3, 1.2 Hz, 1H), 4.26 (d, *J* = 5.1 Hz, 2H), 3.53 (s, 1H). ^{13}C NMR (126 MHz, CDCl$_3$) δ 157.70, 142.41, 138.44, 138.07, 134.64, 130.35, 129.95, 129.12, 128.39, 128.24, 126.21, 125.76, 119.36, 118.13, 116.33, 114.97, 52.35. MS (ESI) calcd for C$_{19}$H$_{16}$N$_4$O, *m/z* 316.1324, found 317.1545 (M+H)[+].

24: (2-(*tert*-butylamino)-7-methyl-3-(pyridin-2-ylamino)furo[2,3-*c*]pyridin-4-yl)methanol—(13 mg, 17%) ^{1}H NMR (400 MHz, MeOD) δ 7.97 (d, *J* = 4.1 Hz, 1H), 7.87 (s, 1H), 7.59 (ddd, *J* = 8.7, 7.2, 1.8 Hz, 1H), 6.75 (ddd, *J* = 7.0, 5.2, 0.7 Hz, 1H), 6.67 (d, *J* = 8.4 Hz, 1H), 4.61 (s, 2H), 2.72 (s, 3H), 1.53 (s, 9H). ^{13}C NMR (126 MHz, MeOD) δ 165.65, 159.92, 147.97, 143.43, 140.55, 139.89, 132.15, 131.86, 125.53, 115.57, 110.65, 96.72, 59.04, 55.33, 30.04, 13.08. MS (ESI) calcd for C$_{18}$H$_{22}$N$_4$O$_2$, *m/z* 326.1743, found 327.1782 (M+H)[+].

25: (2-(*tert*-butylamino)-7-methyl-3-(pyrazin-2-ylamino)furo[2,3-*c*]pyridin-4-yl)methanol—(14 mg, 18%) ^{1}H NMR (500 MHz, MeOD) δ 8.01 (d, *J* = 1.1 Hz, 1H), 7.88 (dd, *J* = 2.8, 1.4 Hz, 1H), 7.80 (s, 1H), 7.77 (d, *J* = 2.8 Hz, 1H), 4.56 (s, 2H), 2.65 (s, 3H),

1.43 (s, 9H). ^{13}C NMR (126 MHz, MeOD) δ 165.60, 156.50, 143.30, 143.00, 140.79, 134.76, 134.39, 132.05, 131.74, 125.39, 95.43, 58.99, 55.50, 29.98, 12.92. MS (ESI) calcd for C$_{17}$H$_{21}$N$_5$O$_2$, *m/z* 327.1695, found 328.1836 (M+H)$^+$.

26: (2-(cyclohexylamino)-7-methyl-3-(pyridin-2-ylamino)furo[2,3-*c*]pyridin-4-yl)methanol—(19 mg, 22%) ^{1}H NMR (500 MHz, MeOD) δ 8.07 (t, *J* = 7.4 Hz, 1H), 7.96 (s, 1H), 7.90 (d, *J* = 5.9 Hz, 1H), 7.29 (d, *J* = 8.4 Hz, 1H), 7.07 (t, *J* = 6.7 Hz, 1H), 4.64 (s, 2H), 3.91 – 3.79 (m, 1H), 2.75 (s, 3H), 2.05 (d, *J* = 8.8 Hz, 2H), 1.87 – 1.77 (m, 2H), 1.68 (d, *J* = 13.1 Hz, 1H), 1.48 – 1.33 (m, 4H), 1.21 (dd, *J* = 12.1, 9.2 Hz, 1H). ^{13}C NMR (126 MHz, MeOD) δ 164.86, 155.98, 145.65, 143.70, 142.10, 137.34, 133.72, 132.85, 124.81, 115.77, 115.45, 89.79, 59.50, 54.25, 34.33, 26.28, 26.16, 12.97. MS (ESI) calcd for C$_{20}$H$_{24}$N$_4$O$_2$, *m/z* 352.1899, found 353.2023 (M+H)$^+$.

27: (2-(cyclohexylamino)-7-methyl-3-(pyrazin-2-ylamino)furo[2,3-*c*]pyridin-4-yl)methanol—(24 mg, 28%) ^{1}H NMR (500 MHz, MeOD) δ 8.10 (s, 1H), 7.97 (d, *J* = 1.4 Hz, 1H), 7.86 (s, 2H), 4.64 (s, 2H), 3.86 – 3.78 (m, 1H), 2.71 (s, 3H), 2.03 – 1.96 (m, 2H), 1.80 (dd, *J* = 5.3, 3.1 Hz, 2H), 1.66 (d, *J* = 13.0 Hz, 1H), 1.38 (t, *J* = 9.6 Hz, 4H), 1.23 – 1.15 (m, 1H). ^{13}C NMR (126 MHz, MeOD) δ 165.01, 156.57, 143.09, 142.98, 141.82, 134.49, 132.10, 131.50, 125.12, 94.07, 58.98, 53.94, 34.42, 26.31, 26.20, 12.80. MS (ESI) calcd for C$_{19}$H$_{23}$N$_5$O$_2$, *m/z* 353.1852, found 354.1902 (M+H)$^+$.

28: (2-(benzylamino)-7-methyl-3-(pyridin-2-ylamino)furo[2,3-*c*]pyridin-4-yl)methanol. (13—mg, 15%) ^{1}H NMR (500 MHz, MeOD) δ 8.06 – 8.01 (m, 1H), 8.00 (s, 1H), 7.89 (d, *J* = 5.9 Hz, 1H), 7.44 – 7.39 (m, 2H), 7.34 (t, *J* = 7.5 Hz, 2H), 7.28 (t, *J* = 7.3 Hz, 1H), 7.23 (d, *J* = 8.6 Hz, 1H), 7.05 (t, *J* = 6.7 Hz, 1H), 4.76 (s, 2H), 4.65 (s, 2H), 2.77 (s, 3H). ^{13}C NMR (126 MHz, MeOD) δ 165.45, 156.13, 145.31, 143.75, 142.15, 138.61, 138.18, 133.67, 133.22, 130.23, 130.00, 129.91, 128.97, 128.77, 125.32, 115.82, 115.01, 90.66, 59.42, 47.33, 12.98. MS (ESI) calcd for C$_{21}$H$_{20}$N$_4$O$_2$, *m/z* 360.1586, found 361.1830 (M+H)$^+$.

29: (2-(benzylamino)-7-methyl-3-(pyrazin-2-ylamino)furo[2,3-*c*]pyridin-4-yl)methanol. (15—mg, 16%) ^{1}H NMR (500 MHz, MeOD) δ 7.99 (s, 1H), 7.94 (dd, *J* = 2.8, 1.5 Hz, 1H), 7.87 (s, 1H), 7.81 (d, *J* = 2.8 Hz, 1H), 7.37 – 7.32 (m, 2H), 7.29 (dd, *J* = 10.3, 5.0 Hz, 2H), 7.21 (t, *J* = 7.3 Hz, 1H), 4.64 (s, 2H), 4.61 (s, 2H), 2.61 (s, 3H). ^{13}C NMR (126 MHz, MeOD) δ 163.44, 156.59, 143.82, 143.17, 139.78, 139.64, 135.93, 134.61, 134.23, 134.16, 129.68, 128.54, 128.38, 125.19, 93.30, 59.41, 47.06, 14.34. MS (ESI) calcd for C$_{20}$H$_{19}$N$_5$O$_2$, *m/z* 361.1539, found 362.1805 (M+H)$^+$.

Synthesis of compound 34: (2-(benzylamino)-7-methyl-3-(phenylamino)furo[2,3-*c*]pyridin- 4-yl)methanol—To a solution of aniline (45 μL, 0.5 mmol) in anhydrous methanol, were added pyridoxal hydrochloride (112 mg, 0.55 mmol), 4N HCl/dioxane (10 μL) and benzyl isonitrile (68 μL, 0.55 mmol). The reaction mixture was then heated under microwave conditions (600 W, 80 °C) in a sealed vial for 2 min. After cooling the reaction mixture to room temperature, the solvents were removed and the residue was purified using column chromatography to obtain compound **34** (84 mg, 47%).^{1}H NMR (500 MHz, MeOD) δ 7.88 (s, 1H), 7.34 (d, *J* = 7.8 Hz, 2H), 7.29 (t, *J* = 7.6 Hz, 2H), 7.21 (t, *J* = 7.2 Hz, 1H), 7.09 (t, *J* = 7.9 Hz, 2H), 6.66 (td, *J* = 7.3, 0.9 Hz, 1H), 6.58 – 6.51 (m, 2H), 4.57 (s, 2H), 4.52 (s, 2H), 2.54 (s, 3H). ^{13}C NMR (126 MHz, MeOD) δ 160.73, 150.14, 141.35, 141.10, 138.40, 137.10, 130.29, 129.51, 128.35, 128.23, 119.02, 114.15, 94.89, 60.27, 47.02, 16.66. MS (ESI) calcd for C$_{22}$H$_{21}$N$_3$O$_2$, *m/z* 359.1634, found 360.1832 (M+H)$^+$.

Synthesis of compound 35: 3-(benzyloxy)-5-(hydroxymethyl)-2-methylisonicotinaldehyde—To a solution of pyridoxalhydrochloride (500 mg, 2.45 mmol) in anhydrous DMF, were added potassium carbonate (408 mg, 2.95 mmol), and benzyl bromide (0.35 mL, 2.95 mmol). The reaction mixture was stirred at room temperature for overnight. After the completion of reaction, water (20 mL) was added and the crude product obtained was extracted in ethyl acetate. The organic layer was washed with water, dried over anhydrous sodium sulfate and evaporated. The residue was purified using column chromatography to obtain compound **35** (100 mg, 15%) ^{1}H NMR (500 MHz, CDCl$_3$) δ 8.05 (s, 1H), 7.45 – 7.32 (m, 5H), 6.64 (d, J = 1.7 Hz, 1H), 5.34 (d, J = 11.2 Hz, 1H), 5.22 (d, J = 12.7 Hz, 1H), 5.19 (d, J = 11.2 Hz, 1H), 4.99 (d, J = 12.7 Hz, 1H), 2.50 (s, 3H). ^{13}C NMR (126 MHz, CDCl$_3$) δ 150.88, 148.63, 136.84, 136.17, 135.53, 135.42, 128.80, 128.47, 127.74, 100.10, 74.13, 69.95, 19.38. MS (ESI) calcd for C$_{15}$H$_{15}$NO$_3$, m/z 257.1052, found 258.1279 (M+H)$^+$.

Synthesis of compound 36: (5-(benzyloxy)-4-(3-(cyclohexylamino)imidazo[1,2-*a*]pyridin-2- yl)-6-methylpyridin-3-yl)methanol—To a solution of 2-aminopyridine (24 mg, 0.25 mmol) in anhydrous acetonitrile, were added 3-(benzyloxy)-5-(hydroxymethyl)-2-methylisonicotinaldehyde **34** (68 mg, 0.28 mmol), 4N HCl/dioxane (5 μL) and cyclohexylisonitrile (30 μL, 0.24 mmol). The reaction mixture was then heated under microwave conditions (400 W, 110 °C) in a sealed vial for 20 min. After cooling the reaction mixture to room temperature, solvents were removed and the residue was purified using column chromatography to obtain compound **36** (19 mg, 17%) ^{1}H NMR (500 MHz, CDCl$_3$) δ 8.41 (s, 1H), 8.07 (d, J = 6.9 Hz, 1H), 7.54 (d, J = 9.1 Hz, 1H), 7.26 – 7.15 (m, 4H), 7.02 – 6.97 (m, 2H), 6.90 (td, J = 6.8, 1.0 Hz, 1H), 4.59 (bs, 1H), 4.43 (s, 2H), 4.36 (bs, 1H), 3.88 (d, J = 7.9 Hz, 1H), 2.61 (bs, 1H), 2.58 (s, 3H), 1.85-1.75 (m, 1H), 1.70-1.65 (m, 1H), 1.50-1.40 (m, 2H), 1.37-1.28 (m, 1H), 1.22-1.05 (s, 2H), 1.05-0.85 (m, 2H), 0.60 (bs, 1H). ^{13}C NMR (126 MHz, CDCl$_3$) δ 152.95, 150.53, 145.20, 141.29, 135.58, 129.62, 129.25, 128.76, 128.58, 128.57, 128.40, 126.28, 125.05, 123.16, 117.47, 112.53, 76.73, 61.64, 56.36, 34.32, 33.74, 25.60, 25.03, 24.53, 19.58. MS (ESI) calcd for C$_{27}$H$_{30}$N$_4$O$_2$, m/z 442.2369, found 443.2410 (M+H)$^+$.

General procedure for the syntheses of compounds 37a-37m

Synthesis of compound 37a: (2-(butylamino)-7-methyl-3-(pyridin-2-ylamino)furo[2,3- *c*]pyridin-4-yl)methanol—To a solution of 2-aminopyridine (24 mg, 0.25 mmol) in anhydrous acetonitrile, were added pyridoxal hydrochloride (56 mg, 0.28 mmol), 4N HCl/dioxane (5 μL) and *n*-butyl isonitrile (25 μL, 0.24 mmol). The reaction mixture was then heated under microwave conditions (600 W, 80 °C) in a sealed vial for 2 min. After cooling the reaction mixture to room temperature, solvents were removed and the residue was purified using column chromatography to obtain compound **37a** (32 mg, 41%) ^{1}H NMR (500 MHz, MeOD) δ 8.06 (t, J = 8.0 Hz, 1H), 7.96 (s, 1H), 7.90 (d, J = 5.8 Hz, 1H), 7.29 (d, J = 8.5 Hz, 1H), 7.07 (t, J = 6.6 Hz, 1H), 4.65 (s, 2H), 3.56 (t, J = 7.1 Hz, 2H), 2.75 (s, 3H), 1.75 – 1.61 (m, 2H), 1.49 – 1.35 (m, 2H), 0.96 (t, J = 7.4 Hz, 3H). ^{13}C NMR (126 MHz, MeOD) δ 165.68, 155.98, 145.61, 143.66, 142.08, 137.58, 133.67, 132.87, 124.84, 115.82, 115.31, 90.01, 59.50, 43.64, 32.79, 20.93, 13.99, 12.96. MS (ESI) calcd for C$_{18}$H$_{22}$N$_4$O$_2$, m/z 326.1743, found 327.1925 (M+H)$^+$.

Compounds **37b**-**37m** were synthesized similarly as compound **37a**.

37b: (7-methyl-2-(pentylamino)-3-(pyridin-2-ylamino)furo[2,3-*c*]pyridin-4-yl)methanol—(27 mg, 33%) ^{1}H NMR (500 MHz, MeOD) δ 8.06 (t, J = 8.0 Hz, 1H), 7.96 (s, 1H), 7.91 (d, J = 5.9 Hz, 1H), 7.28 (d, J = 8.5 Hz, 1H), 7.07 (t, J = 6.6 Hz, 1H), 4.65 (s, 2H), 3.56 (t, J = 7.1 Hz, 2H), 2.75 (s, 3H), 1.75 – 1.64 (m, 2H), 1.38 (d, J = 3.6 Hz, 4H),

0.92 (t, *J* = 6.9 Hz, 3H). ^{13}C NMR (126 MHz, MeOD) δ 165.68, 156.04, 145.55, 143.66, 142.09, 137.74, 133.66, 132.85, 124.85, 115.82, 115.25, 90.09, 59.49, 43.90, 30.42, 29.98, 23.31, 14.32, 12.95. MS (ESI) calcd for $C_{19}H_{24}N_4O_2$, *m/z* 340.1899, found 341.2058 (M +H)[+].

37c: (2-(isopropylamino)-7-methyl-3-(pyridin-2-ylamino)furo[2,3-*c*]pyridin-4-yl)methanol—(20 mg, 27%) ^{1}H NMR (500 MHz, MeOD) δ 8.05 (t, *J* = 8.0 Hz, 1H), 7.95 (s, 1H), 7.90 (d, *J* = 5.9 Hz, 1H), 7.26 (d, *J* = 8.6 Hz, 1H), 7.05 (t, *J* = 6.7 Hz, 1H), 4.63 (s, 2H), 4.25 (dt, *J* = 13.0, 6.5 Hz, 1H), 2.74 (s, 3H), 1.33 (d, *J* = 6.5 Hz, 6H). ^{13}C NMR (126 MHz, MeOD) δ 164.96, 156.16, 145.41, 143.72, 142.06, 137.79, 133.63, 132.82, 124.86, 115.77, 115.24, 90.04, 59.48, 47.16, 23.12, 12.94. MS (ESI) calcd for $C_{17}H_{20}N_4O_2$, *m/z* 312.1586, found 313.1740 (M+H)[+].

37d: (7-methyl-2-(pentan-2-ylamino)-3-(pyridin-2-ylamino)furo[2,3-*c*]pyridin-4-yl)methanol—(34 mg, 42%) ^{1}H NMR (500 MHz, MeOD) δ 7.99 (t, *J* = 8.0 Hz, 1H), 7.88 (s, 1H), 7.83 (d, *J* = 5.2 Hz, 1H), 7.20 (d, *J* = 7.3 Hz, 1H), 7.00 (t, *J* = 6.7 Hz, 1H), 4.56 (s, 2H), 4.03 (dq, *J* = 12.9, 6.5 Hz, 1H), 2.66 (s, 3H), 1.60 – 1.41 (m, 2H), 1.38 – 1.26 (m, 2H), 1.23 (d, *J* = 6.6 Hz, 3H), 0.86 (t, *J* = 7.4 Hz, 3H). ^{13}C NMR (126 MHz, MeOD) δ 165.14, 155.98, 145.72, 143.66, 142.17, 137.38, 133.77, 132.84, 124.79, 115.82, 115.41, 89.73, 59.52, 51.18, 39.97, 21.53, 20.53, 14.15, 12.94. MS (ESI) calcd for $C_{19}H_{24}N_4O_2$, *m/z* 340.1899, found 341.2077 (M+H)[+].

37e: (7-methyl-3-(pyridin-2-ylamino)-2-((2,4,4-trimethylpentan-2-yl)amino)furo[2,3-*c*]pyridin-4-yl)methanol—(33 mg, 36%) ^{1}H NMR (500 MHz, MeOD) δ 8.08 (t, *J* = 8.0 Hz, 1H), 7.99 (s, 1H), 7.90 (s, 1H), 7.27 (s, 1H), 7.08 (dd, *J* = 7.0, 6.4 Hz, 1H), 4.63 (s, 2H), 2.78 (s, 3H), 1.95 (d, *J* = 12.9 Hz, 2H), 1.60 (s, 6H), 1.00 (s, 9H). ^{13}C NMR (126 MHz, MeOD) δ 165.37, 156.14, 145.64, 143.96, 141.40, 137.05, 133.87, 132.93, 124.92, 115.77, 115.62, 90.82, 59.88, 59.51, 53.31, 32.62, 31.82, 30.73, 13.06. MS (ESI) calcd for $C_{22}H_{30}N_4O_2$, *m/z* 382.2369, found 383.2541 (M+H)[+].

37f: (7-methyl-3-(pyridin-2-ylamino)-2-(((trimethylsilyl)methyl)amino)furo[2,3-*c*]pyridin-4-yl)methanol—(24 mg, 28%) ^{1}H NMR (500 MHz, MeOD) δ 8.03 (t, *J* = 8.0 Hz, 1H), 7.91-7.90 (m, 2H), 7.24 (d, *J* = 8.7 Hz, 1H), 7.04 (t, *J* = 6.6 Hz, 1H), 4.62 (s, 2H), 3.11 (s, 2H), 2.72 (s, 3H), 0.12 (s, 9H). ^{13}C NMR (126 MHz, MeOD) δ 165.66, 156.25, 145.27, 143.32, 142.02, 138.19, 133.57, 132.16, 124.28, 115.77, 115.00, 90.25, 59.52, 34.64, 12.94, -2.60. MS (ESI) calcd for $C_{18}H_{24}N_4O_2Si$, *m/z* 356.1669, found 357.1815 (M +H)[+].

37g: (7-methyl-2-((2-morpholinoethyl)amino)-3-(pyridin-2-ylamino)furo[2,3-*c*]pyridin-4-yl)methanol—(9 mg, 10%) ^{1}H NMR (500 MHz, MeOD) δ 8.03 (s, 2H), 7.93 (d, *J* = 5.8 Hz, 1H), 7.27 (d, *J* = 7.3 Hz, 1H), 7.05 (t, *J* = 6.5 Hz, 1H), 4.66 (s, 2H), 4.06-3.95 (m, 6H), 3.54 (bs, 2H), 3.42 (bs, 4H), 2.80 (s, 3H). ^{13}C NMR (126 MHz, MeOD) δ 165.51, 156.26, 145.10, 143.92, 141.95, 138.27, 134.09, 133.62, 126.01, 115.97, 115.07, 90.35, 64.80, 59.39, 57.37, 53.45, 37.84, 13.21. MS (ESI) calcd for $C_{20}H_{25}N_5O_3$, *m/z* 383.1957, found 384.2132 (M+H)[+].

37h: Ethyl 2-((4-(hydroxymethyl)-7-methyl-3-(pyridin-2-ylamino)furo[2,3-*c*]pyridin-2-yl)amino)acetate—(21 mg, 25%) ^{1}H NMR (500 MHz, MeOD) δ 8.07 (t, *J* = 8.0 Hz, 1H), 8.03 (s, 1H), 7.91 (d, *J* = 6.1 Hz, 1H), 7.29 (d, *J* = 8.9 Hz, 1H), 7.08 (t, *J* = 6.7 Hz, 1H), 4.66 (s, 2H), 4.36 (s, 2H), 4.18 (q, *J* = 7.1 Hz, 2H), 2.74 (s, 3H), 1.25 (t, *J* = 7.1 Hz, 3H). ^{13}C NMR (126 MHz, MeOD) δ 170.68, 165.42, 155.75, 145.81, 143.87, 142.15,

137.71, 133.94, 133.89, 125.93, 115.98, 115.25, 91.02, 62.95, 59.42, 44.55, 14.48, 13.03. MS (ESI) calcd for $C_{18}H_{20}N_4O_4$, *m/z* 356.1485, found 357.1738 (M+H)$^+$.

37i: *tert*-butyl 3-((4-(hydroxymethyl)-7-methyl-3-(pyridin-2-ylamino)furo[2,3-*c*]pyridin-2- yl)amino)propanoate—(20 mg, 21%) ^{1}H NMR (500 MHz, MeOD) δ 8.08 (t, *J* = 8.0 Hz, 1H), 8.00 (s, 1H), 7.91 (d, *J* = 5.8 Hz, 1H), 7.29 (d, *J* = 7.8 Hz, 1H), 7.08 (t, *J* = 6.7 Hz, 1H), 4.66 (s, 2H), 3.80 (t, *J* = 6.4 Hz, 2H), 2.78 (s, 3H), 2.67 (t, *J* = 6.7 Hz, 2H), 1.42 (s, 9H). ^{13}C NMR (126 MHz, MeOD) δ 171.99, 165.49, 155.86, 145.77, 143.76, 142.08, 137.49, 133.79, 133.30, 125.17, 115.86, 115.36, 90.25, 82.28, 59.49, 39.67, 36.03, 28.31, 13.02. MS (ESI) calcd for $C_{21}H_{26}N_4O_4$, *m/z* 398.1954, found 399.2128 (M+H)$^+$.

37j: Diethyl (((4-(hydroxymethyl)-7-methyl-3-(pyridin-2-ylamino)furo[2,3-*c*]pyridin-2- yl)amino)methyl)phosphonate—(13 mg, 13%) ^{1}H NMR (500 MHz, MeOD) δ 8.08 – 8.00 (m, 2H), 7.95 (d, *J* = 5.7 Hz, 1H), 7.23 (d, *J* = 4.9 Hz, 1H), 7.06 (t, *J* = 6.5 Hz, 1H), 4.69 (s, 2H), 4.24 – 4.16 (m, 4H), 4.09 (d, *J* = 10.6 Hz, 2H), 2.81 (s, 3H), 1.33 (t, *J* = 7.0 Hz, 6H). ^{13}C NMR (126 MHz, MeOD) δ 164.98, 156.41, 145.04, 143.68, 142.06, 139.12, 133.83, 133.71, 125.96, 115.97, 114.67, 91.93, 64.56 (d, *J* = 6.9 Hz), 59.37, 39.02 (d, *J* = 158.9 Hz), 16.78 (d, *J* = 5.6 Hz), 13.09. MS (ESI) calcd for $C_{19}H_{25}N_4O_5P$, *m/z* 420.1563, found 421.1672 (M+H)$^+$.

37k: (2-((4-methoxyphenyl)amino)-7-methyl-3-(pyridin-2-ylamino)furo[2,3-*c*]pyridin-4- yl)methanol—(13 mg, 14%) ^{1}H NMR (500 MHz, MeOD) δ 7.99 – 7.87 (m, 2H), 7.62 (t, *J* = 7.8 Hz, 1H), 7.33 (d, *J* = 8.8 Hz, 2H), 6.90 (d, *J* = 8.8 Hz, 2H), 6.77 (t, *J* = 6.3 Hz, 2H), 4.66 (s, 2H), 3.77 (s, 3H), 2.71 (s, 3H). ^{13}C NMR (126 MHz, MeOD) δ 162.79, 159.21, 158.92, 146.57, 143.34, 141.31, 140.61, 132.84, 132.22, 130.80, 126.51, 124.33, 115.64, 115.43, 111.46, 96.53, 62.30, 58.97, 55.97, 13.06. MS (ESI) calcd for $C_{21}H_{20}N_4O_3$, *m/z* 376.1535, found 377.1694 (M+H)$^+$.

37l: (2-((2-chloro-6-methylphenyl)amino)-7-methyl-3-(pyridin-2-ylamino)furo[2,3- *c*]pyridin-4-yl)methanol—(27 mg, 28%) ^{1}H NMR (500 MHz, MeOD) δ 8.10 (s, 1H), 7.90 (dd, *J* = 20.4, 6.6 Hz, 2H), 7.28 – 7.15 (m, 3H), 7.03 (t, *J* = 6.6 Hz, 1H), 6.95 (s, 1H), 4.70 (s, 2H), 2.75 (s, 3H), 2.32 (s, 3H). ^{13}C NMR (126 MHz, MeOD) δ 162.57, 155.17, 145.80, 144.21, 142.68, 139.93, 136.98, 134.45, 133.96, 133.78, 132.14, 130.74, 128.65, 126.80, 115.93, 114.82, 91.45, 59.30, 18.71, 13.11. MS (ESI) calcd for $C_{21}H_{19}ClN_4O_2$, *m/z* 394.1197, found 395.1349 (M+H)$^+$.

37m: (*S*)-(7-methyl-2-((1-phenylethyl)amino)-3-(pyridin-2-ylamino)furo[2,3-*c*]pyridin-4- yl)methanol—(28 mg, 31%) ^{1}H NMR (500 MHz, MeOD) δ 7.92 (s, 1H), 7.89 (t, *J* = 8.0 Hz, 1H), 7.90 – 7.81 (m, 1H), 7.38 (d, *J* = 7.6 Hz, 2H), 7.29 (t, *J* = 7.4 Hz, 2H), 7.21 (t, *J* = 7.2 Hz, 1H), 7.05 (d,*J* = 6.1 Hz, 1H), 6.94 (t, *J* = 6.4 Hz, 1H), 5.20 (q, *J* = 6.8 Hz, 1H), 4.58 (s, 2H), 2.68 (s, 3H), 1.60 (d, *J* = 6.9 Hz, 3H). ^{13}C NMR (126 MHz, MeOD) δ 164.81, 157.13, 144.72, 143.97, 143.61, 142.11, 140.61, 133.20, 132.80, 129.92, 128.71, 126.98, 125.52, 115.70, 113.93, 91.91, 59.24, 54.49, 23.31, 12.88. MS (ESI) calcd for $C_{22}H_{22}N_4O_2$, *m/z* 374.1743, found 375.1931 (M+H)$^+$.

Synthesis of compound (37n): ((2-amino-7-methyl-3-(pyridin-2-ylamino)furo[2,3-*c*]pyridin- 4-yl)methanol—The solution of compound **37e** (95 mg, 0.25 mmol) in TFA/CH$_2$Cl$_2$ (50%, 4 mL) was stirred at room temperature for 6 h. The solvents were removed and the residue obtained was column purified to afford compound **37n** (56 mg, 84%).^{1}H NMR (500 MHz, MeOD) δ 7.91 – 7.86 (m, 2H), 7.81 (t, *J* = 7.9 Hz, 1H), 6.96 (d, *J* = 8.6 Hz, 1H), 6.87 (t, *J* = 6.5 Hz, 1H), 4.61 (s, 2H), 2.66 (s, 3H). ^{13}C NMR (126 MHz, MeOD) δ 167.39, 157.68, 143.36, 143.14, 142.12, 132.82, 132.44, 125.47,

115.59, 113.10, 92.54, 59.18, 12.80. MS (ESI) calcd for $C_{14}H_{14}N_4O_2$, *m/z* 270.1117, found 271.1310 (M+H)[+].

Compounds **38a**-**38c** were synthesized similarly as compound **34**.

38a: (7-methyl-2-(pentylamino)-3-(phenylamino)furo[2,3-*c*]pyridin-4-yl)methanol—

(117 mg, 70%) ^{1}H NMR (500 MHz, MeOD) δ 7.85 (s, 1H), 7.14 (dd, *J* = 8.6, 7.4 Hz, 2H), 6.71 (tt, *J* = 7.4, 1.0 Hz, 1H), 6.60 (dd, *J* = 8.6, 1.0 Hz, 2H), 4.65 – 4.59 (m, 2H), 3.51 (t, *J* = 7.1 Hz, 2H), 2.68 (s, 3H), 1.72 – 1.57 (m, 2H), 1.41 – 1.28 (m, 4H), 0.95 – 0.84 (m, 3H). ^{13}C NMR (126 MHz, MeOD) δ 165.54, 149.56, 143.22, 141.35, 133.46, 132.44, 130.44, 125.33, 119.45, 114.08, 96.74, 59.31, 43.42, 31.00, 29.94, 23.33, 14.34, 13.48. MS (ESI) calcd for $C_{20}H_{25}N_3O_2$, *m/z* 339.1947, found 340.2087 (M+H)[+].

38b: (3-((3-fluorophenyl)amino)-7-methyl-2-(pentylamino)furo[2,3-*c*]pyridin-4-yl) methanol—

(70 mg, 82%) ^{1}H NMR (500 MHz, MeOD) δ 7.81 (s, 1H), 7.06 (td, *J* = 8.2, 6.7 Hz, 1H), 6.42 – 6.32 (m, 2H), 6.23 (d, *J* = 11.5 Hz, 1H), 4.60 (s, 2H), 3.46 (t, *J* = 7.1 Hz, 2H), 2.65 (s, 3H), 1.59 (p, *J* = 7.1 Hz, 2H), 1.31 – 1.23 (m, 4H), 0.83 (t, *J* = 7.0 Hz, 3H). ^{13}C NMR (126 MHz, MeOD) 166.34, 165.62 (d, *J* = 242.1 Hz), 151.55 (d, *J* = 10.4 Hz), 142.79, 142.04, 131.84 (d, *J* = 10.1 Hz), 131.65, 131.28, 125.42, 110.01, 105.58 (d, *J* = 21.8 Hz), 100.74 (d, *J* = 25.8 Hz), 96.47, 58.95, 43.43, 30.83, 29.93, 23.33, 14.35, 12.79. MS (ESI) calcd for $C_{20}H_{24}FN_3O_2$, *m/z* 357.1853, found 358.2013 (M+H)[+].

38c: (7-methyl-3-((3-nitrophenyl)amino)-2-(pentylamino)furo[2,3-*c*]pyridin-4-yl)methanol—

(34 mg, 37%) ^{1}H NMR (500 MHz, MeOD) δ 7.90 (s, 1H), 7.49 (dd, *J* = 8.1, 2.2 Hz, 1H), 7.34 (s, 1H), 7.31 (t, *J* = 8.1 Hz, 1H), 6.95 (d, *J* = 8.0 Hz, 1H), 4.54 (s, 2H), 3.41 (t, *J* = 7.0 Hz, 2H), 2.56 (s, 3H), 1.65 – 1.52 (m, 2H), 1.30 (dd, *J* = 8.5, 4.8 Hz, 4H), 0.86 (t, *J* = 6.5 Hz, 3H). ^{13}C NMR (126 MHz, MeOD) δ 160.86, 151.59, 150.89, 144.93, 141.84, 138.47, 136.71, 131.12, 124.51, 120.06, 113.05, 107.81, 92.23, 60.13, 43.34, 31.50, 30.02, 23.40, 16.73, 14.35. MS (ESI) calcd for $C_{20}H_{24}N_4O_4$, *m/z* 384.1798, found 385.1950 (M+H)[+].

Synthesis of compound (39): 2,2′-(hexane-1,6-diylbis(azanediyl))bis(7-methyl-3-(pyridin-2- ylamino)furo[2,3-*c*]pyridine-4,2-diyl))dimethanol—

To a solution of 2-aminopyridine (48 mg, 0.50 mmol) in anhydrous acetonitrile, were added pyridoxalhydrochloride (112 mg, 0.56 mmol), 4N HCl/dioxane (10 μL) and 1,6-diisocyanohexane (36 μL, 0.24 mmol). The reaction mixture was then heated under microwave conditions (600 W, 80 °C) in a sealed vial for 2 min. After cooling the reaction mixture to room temperature, solvent was removed and the residue was purified using column chromatography to obtain compound **39** (21 mg, 7%). ^{1}H NMR (500 MHz, MeOD) δ 8.07 (t, *J* = 8.0 Hz, 2H), 7.97 (s, 2H), 7.90 (d, *J* = 5.6 Hz, 2H), 7.31 (d, *J* = 5.6 Hz, 2H), 7.07 (t, *J* = 6.7 Hz, 2H), 4.64 (s, 4H), 3.57 (t, *J* = 7.0 Hz, 4H), 2.75 (s, 6H), 1.78 – 1.65 (m, 4H), 1.46 (s, 4H). ^{13}C NMR (126 MHz, MeOD) δ 165.67, 155.95, 145.66, 143.71, 142.10, 137.48, 133.70, 132.91, 124.87, 115.83, 115.43, 90.05, 59.50, 43.86, 30.65, 27.48, 13.02. MS (ESI) calcd for $C_{34}H_{38}N_8O_4$, *m/z* 622.3016, found 623.3187 (M+H)[+].

X-ray crystallographic structural studies of 20, 28, and 37e—

Crystals for compound **28** utilize the non-centrosymmetric triclinic space group P1-C1 with eight crystallographically-independent molecules in the asymmetric unit. They also invariably form multiply-twinned bundles. After many unsuccessful attempts, a multi-domain specimen of **28** was cut from one of these bundles that gave a set of diffracted intensities that permitted a crystal structure solution but not a satisfactory refinement. Full sets of unique diffracted intensities were measured for single-domain specimens of compounds **20**

and **37e** using monochromated CuKα radiation (λ= 1.54178 Å) on a Bruker Proteum Single Crystal Diffraction System equipped with Helios multilayer optics, an APEX II CCD detector and a Bruker MicroStar microfocus rotating anode x-ray source operating at 45kV and 60mA. Diffracted intensities were obtained with the Bruker program SAINT and the structures were solved using "direct methods" techniques incorporated into the Bruker SHELXTL Version 2010.3-0 software package. All stages of weighted full-matrix least-squares refinement were performed using the SHELXTL software with F_o^2 data. The final structural model for compounds **20** and **37e** incorporated anisotropic thermal parameters for all non-hydrogen atoms and isotropic thermal parameters for all hydrogen atoms. The respective asymmetric units consist of four molecules of **20**; one molecule of **37e**. All hydrogen atoms for **37e** and hydrogen atoms of **20** that are bonded to amine nitrogens (one in each molecule) were located in a difference Fourier map and included in the structural model as independent isotropic atoms whose parameters were allowed to vary in least-squares refinement cycles. All hydroxyl hydrogens for **20** were placed at idealized sp^3-hybridized positions with an O-H bond length of 0.84 Å; the hydroxyl group was then allowed to rotate about its O-C bond during least squares refinement cycles. The remaining hydrogen atoms for **20** were included in the structural model as idealized atoms (assuming sp^2- or sp^3-hybridization of the carbon or nitrogen atoms and C-H bond lengths of 0.95 to 1.00 Å or N-H bond lengths of 0.88 Å). The isotropic thermal parameters of all idealized hydrogen atoms for **20** were fixed at values 1.2 (nonmethyl) or 1.5 (methyl) times the equivalent isotropic thermal parameter of the carbon, nitrogen or oxygen atom to which they are covalently bonded.

Human TLR-3/-4/-5/-7/-8/-9 Reporter Gene assays (NF-κB induction)—The induction of NF- κB was quantified using human TLR-3/-4/-5/-7/-8/-9-specific HEK-Blue™ reporter gene assays as previously described by us.[27,40,49] HEK293 cells stably co-transfected with the appropriate hTLR and secreted alkaline phosphatase (sAP) were maintained in HEK-Blue™ Selection medium containing zeocin and normocin. Stable expression of secreted alkaline phosphatase (sAP) under control of NF-κB/AP-1 promoters is inducible by appropriate TLR agonists, and extracellular sAP in the supernatant is proportional to NF-κB induction. HEK-Blue™ cells were incubated at a density of ~10^5 cells/mL in a volume of 80 WL/well, in 384-well, flat-bottomed, cell culture-treated microtiter plates until confluency was achieved, and subsequently stimulated with graded concentrations of stimuli. sAP was assayed spectrophotometrically using an alkaline phosphatase-specific chromogen (present in HEK-detection medium as supplied by the vendor) at 620 nm.

Immunoassays for cytokines—Fresh human peripheral blood mononuclear cells (hPBMC) were isolated from human blood obtained by venipuncture with informed consent and as per institutional guidelines on Ficoll-Hypaque gradients as described elsewhere.[55] Aliquots of PBMCs (10^5 cells in 100 μL/well) were stimulated for 12 h with graded concentrations of test compounds. Supernatants were isolated by centrifugation, and were assayed in triplicates using analyte-specific multiplexed cytokine/chemokine bead array assays as reported by us previously.[56]

Transcriptomal profiling in human PBMCs—Detailed procedures for transcriptomal profiling have been described by us previously.[49] Briefly, fresh human PBMC samples were stimulated with 10 μg/mL of **37b** and **37f** for two hours, and total RNA was extracted from treated and negative control blood samples with QIAamp RNA Blood Mini Kit (Qiagen). Subsequently, 160 ng of each of the RNA samples was used. The Human Genome GeneChip U133 plus 2.0 oligonucleotide array (Affymetrix, Santa Clara, CA) was employed. Established standard protocols at the KU Genomics Facility were performed on

cRNA target preparation, array hybridization, washing, staining and image scanning. The microarray data was first subjected to quality assessment using the Affymetrix GeneChip Operating Software (GCOS). QC criteria included low background, low noise, detection of positive controls, and a $5'/3'$ ratio of < 3.0. To facilitate direct comparison of gene expression data between different samples, the GeneChip data were first subjected to preprocessing. This step involved scaling (in GCOS) data from all chips to a target intensity value of 500, and further normalizations steps in GeneSpring GX (Agilent Technologies, Santa Clara, CA). Prior to identifying target genes, genes that were detected as non-expressed in all samples, i.e., those with absence calls, were filtered out. To identify genes whose expression was changed by our compounds, a fold change threshold of 2.0 between the compound treatment and the negative control was used.

Rabbit immunization and antigen-specific ELISA—All experiments were performed at Harlan Laboratories (Indianapolis, IN) in accordance with institutional guidelines (University of Kansas IACUC permit # 119-06). Cohorts of adult female New Zealand White rabbits (n = 4 per cohort) were immunized intramuscularly in the flank region with either 100 μg of bovine α-lactalbumin in 0.2 mL saline (unadjuvanted control), or 100 μg of bovine α-lactalbumin plus 100 μg of **37b**, **40**, or **41** in 0.2 mL saline. Pre-immune test-bleeds were first obtained via venipuncture of the marginal vein of the ear. Animals were immunized on Days 1, 15 and 28. A final test-bleed was performed via the marginal vein of the ear on Day 38. Sera were stored at -80 °C until used. Bovine α-lactalbumin-specific ELISAs were performed in 384-well format using automated liquid handling methods as described by us.[42]

Supplementary Material

Refer to Web version on PubMed Central for supplementary material.

Acknowledgments

Abbreviations used

dsRNA	double-stranded RNA
EC$_{50}$	Half-maximal effective concentration
ESI-TOF	Electrospray ionization-time of flight
HEK	Human embryonic kidney
IL	Interleukin
LPS	Lipopolysaccharides
MHC	Major histocompatibility complex
MyD88	myeloid differentiation primary response gene 88
NF-κB	Nuclear factor-κB
PAMPs	Pathogen associated molecular patterns
PBMCs	Peripheral blood mononuclear cells
PRRs	Pattern recognition receptors

SAP	Secreted alkaline phosphatase
SAR	Structure activity relationship
ssRNA	singlestranded RNA
TLR	Toll like receptor
TNF-α	Tumor necrosis factor-α

References

1. Iwasaki A, Medzhitov R. Regulation of adaptive immunity by the innate immune system. Science. 2010; 327:291–295. [PubMed: 20075244]

2. Iwasaki A, Medzhitov R. Toll-like receptor control of the adaptive immune responses. Nat Immunol. 2004; 5:987–995. [PubMed: 15454922]

3. Janeway CA Jr, Medzhitov R. Innate immune recognition. Annu Rev Immunol. 2002; 20:197–216. [PubMed: 11861602]

4. Lee MS, Kim YJ. Pattern-recognition receptor signaling initiated from extracellular, membrane, and cytoplasmic space. Mol Cells. 2007; 23:1–10. [PubMed: 17464205]

5. Seaton BA, Crouch EC, McCormack FX, Head JF, Hartshorn KL, Mendelsohn R. Review: Structural determinants of pattern recognition by lung collectins. Innate Immun. 2010; 16:143–150. [PubMed: 20423923]

6. Runza VL, Schwaeble W, Mannel DN. Ficolins: novel pattern recognition molecules of the innate immune response. Immunobiol. 2008; 213:297–306.

7. Agrawal A, Singh PP, Bottazzi B, Garlanda C, Mantovani A. Pattern recognition by pentraxins. Adv Exp Med Biol. 2009; 653:98–116. [PubMed: 19799114]

8. Bianchi ME. DAMPs, PAMPs and alarmins: all we need to know about danger. J Leukoc Biol. 2007; 81:1–5. [PubMed: 17032697]

9. Yoneyama M, Fujita T. Function of RIG-I-like receptors in antiviral innate immunity. J Biol Chem. 2007; 282:15315–15318. [PubMed: 17395582]

10. Shaw MH, Reimer T, Kim YG, Nunez G. NOD-like receptors (NLRs): bona fide intracellular microbial sensors. Curr Opin Immunol. 2008; 20:377–382. [PubMed: 18585455]

11. Kawai T, Akira S. The role of pattern-recognition receptors in innate immunity: update on Toll-like receptors. Nat Immunol. 2010; 11:373–384. [PubMed: 20404851]

12. Kumagai Y, Takeuchi O, Akira S. Pathogen recognition by innate receptors. J Infect Chemother. 2008; 14:86–92. [PubMed: 18622669]

13. Takeda K, Akira S. Toll-like receptors. Curr Protoc Immunol. 2007; Chapter 14(Unit)

14. Akira S. Toll-like receptors and innate immunity. Adv Immunol. 1902; 78:1–56. [PubMed: 11432202]

15. Akira S, Takeda K, Kaisho T. Toll-like receptors: critical proteins linking innate and acquired immunity. Nature Immunol. 2001; 2:675–680. [PubMed: 11477402]

16. Cottalorda A, Verschelde C, Marcais A, Tomkowiak M, Musette P, Uematsu S, Akira S, Marvel J, Bonnefoy-Berard N. TLR2 engagement on CD8 T cells lowers the threshold for optimal antigen-induced T cell activation. Eur J Immunol. 2006; 36:1684–1693. [PubMed: 16761317]

17. Kaisho T, Akira S. Toll-like receptors as adjuvant receptors. Biochim Biophys Acta. 2002; 1589:1–13. [PubMed: 11909637]

18. Wu W, Li R, Malladi SS, Warshakoon HJ, Kimbrell MR, Amolins MW, Ukani R, Datta A, David SA. Structure-activity relationships in toll-like receptor-2 agonistic diacylthioglycerol lipopeptides. J Med Chem. 2010; 53:3198– 3213. [PubMed: 20302301]

19. Agnihotri G, Crall BM, Lewis TC, Day TP, Balakrishna R, Warshakoon HJ, Malladi SS, David SA. Structure-activity relationships in toll-like receptor 2-agonists leading to simplified monoacyl lipopeptides. J Med Chem. 2011; 54:8148–8160. [PubMed: 22007676]

20. Salunke DB, Shukla NM, Yoo E, Crall BM, Balakrishna R, Malladi SS, David SA. Structure-Activity Relationships in Human Toll-like Receptor 2- Specific Monoacyl Lipopeptides. J Med Chem. 2012; 55:3353–3363. [PubMed: 22385476]

21. Liu L, Botos I, Wang Y, Leonard JN, Shiloach J, Segal DM, Davies DR. Structural basis of toll-like receptor 3 signaling with double-stranded RNA. Science. 2008; 320:379–381. [PubMed: 18420935]

22. Uematsu S, Akira S. Toll-like receptors and Type I interferons. J Biol Chem. 2007; 282:15319–15323. [PubMed: 17395581]

23. Rietschel ET, Brade H, Brade L, Brandenburg K, Schade UF, Seydel U, Z„hringer U, Galanos C, Lüderitz O, Westphal O, Labischinski H, Kusumoto S, Shiba T. Lipid A, the endotoxic center of bacterial lipopolysaccharides: Relation of chemical structure to biological activity. Prog Clin Biol Res. 1987; 231:25–53. [PubMed: 3588622]

24. Bowen WS, Minns LA, Johnson DA, Mitchell TC, Hutton MM, Evans JT. Selective TRIF-dependent signaling by a synthetic toll-like receptor 4 agonist. Sci Signal. 2012; 5:ra13. [PubMed: 22337809]

25. Stover AG, Da Silva CJ, Evans JT, Cluff CW, Elliott MW, Jeffery EW, Johnson DA, Lacy MJ, Baldridge JR, Probst P, Ulevitch RJ, Persing DH, Hershberg RM. Structure-activity relationship of synthetic toll-like receptor 4 agonists. J Biol Chem. 2004; 279:4440–4449. [PubMed: 14570885]

26. Gerster JF, Lindstrom KJ, Miller RL, Tomai MA, Birmachu W, Bomersine SN, Gibson SJ, Imbertson LM, Jacobson JR, Knafla RT, Maye PV, Nikolaides N, Oneyemi FY, Parkhurst GJ, Pecore SE, Reiter MJ, Scribner LS, Testerman TL, Thompson NJ, Wagner TL, Weeks CE, Andre JD, Lagain D, Bastard Y, Lupu M. Synthesis and structureactivity- relationships of 1H-imidazo[4,5-c]quinolines that induce interferon production. J Med Chem. 2005; 48:3481–3491. [PubMed: 15887957]

27. Shukla NM, Malladi SS, Mutz CA, Balakrishna R, David SA. Structureactivity relationships in human toll-like receptor 7-active imidazoquinoline analogues. J Med Chem. 2010; 53:4450–4465. [PubMed: 20481492]

28. Shukla NM, Mutz CA, Malladi SS, Warshakoon HJ, Balakrishna R, David SA. Toll-Like Receptor (TLR)-7 and -8 Modulatory Activities of Dimeric Imidazoquinolines. J Med Chem. 2012; 55:1106–1116. [PubMed: 22239408]

29. Hamilton RD, Wynalda MA, Fitzpatrick FA, Teagarden DL, Hamdy AH, Snider BG, Weed SD, Stringfellow DA. Comparison between circulating interferon and drug levels following administration of 2-amino-5- bromo-6-phenyl-4(3H)-pyrimidinone (ABPP) to different animal species. J Interferon Res. 1982; 2:317–327. [PubMed: 6182250]

30. Stringfellow DA. Comparation interferon- inducing and antiviral properties of 2-amino- 5-bromo-6-methyl-4-pyrimidinol (U-25,166), tilorone hydrochloride, and polyinosinic-polycytidylic acid. Antimicrob Agents Chemother. 1977; 11:984–992. [PubMed: 879763]

31. Lee J, Chuang TH, Redecke V, She L, Pitha PM, Carson DA, Raz E, Cottam HB. Molecular basis for the immunostimulatory activity of guanine nucleoside analogs: activation of Toll-like receptor 7. Proc Natl Acad Sci U S A. 2003; 100:6646–6651. [PubMed: 12738885]

32. Hirota K, Kazaoka K, Niimoto I, Kumihara H, Sajiki H, Isobe Y, Takaku H, Tobe M, Ogita H, Ogino T, Ichii S, Kurimoto A, Kawakami H. Discovery of 8-hydroxyadenines as a novel type of interferon inducer. J Med Chem. 2002; 45:5419–5422. [PubMed: 12459008]

33. Isobe Y, Tobe M, Ogita H, Kurimoto A, Ogino T, Kawakami H, Takaku H, Sajiki H, Hirota K, Hayashi H. Synthesis and structure-activity relationships of 2-substituted-8-hydroxyadenine derivatives as orally available interferon inducers without emetic side effects. Bioorg Med Chem. 2003; 11:3641–3647. [PubMed: 12901909]

34. Gorden KB, Gorski KS, Gibson SJ, Kedl RM, Kieper WC, Qiu X, Tomai MA, Alkan SS, Vasilakos JP. Synthetic TLR agonists reveal functional differences between human TLR7 and TLR8. J Immunol. 2005; 174:1259–1268. [PubMed: 15661881]

35. Gorski KS, Waller EL, Bjornton-Severson J, Hanten JA, Riter CL, Kieper WC, Gorden KB, Miller JS, Vasilakos JP, Tomai MA, Alkan SS. Distinct indirect pathways govern human NK-cell activation by TLR-7 and TLR-8 agonists. Int Immunol. 2006; 18:1115–1126. [PubMed: 16728430]

36. Jin MS, Lee JO. Structures of TLR-ligand complexes. Curr Opin Immunol. 2008; 20:414–419. [PubMed: 18585456]

37. Yoon SI, Kurnasov O, Natarajan V, Hong M, Gudkov AV, Osterman AL, Wilson IA. Structural basis of TLR5-flagellin recognition and signaling. Science. 2012; 335:859–864. [PubMed: 22344444]

38. Petrone PM, Simms B, Nigsch F, Lounkine E, Kutchukian P, Cornett A, Deng Z, Davies JW, Jenkins JL, Glick M. Rethinking Molecular Similarity: Comparing Compounds on the Basis of Biological Activity. ACS Chem Biol. 201210.1021/cb3001028

39. Tsunoyama K, Amini A, Sternberg MJ, Muggleton SH. Scaffold hopping in drug discovery using inductive logic programming. J Chem Inf Model. 2008; 48:949–957. [PubMed: 18457387]

40. Shukla NM, Kimbrell MR, Malladi SS, David SA. Regioisomerismdependent TLR7 agonism and antagonism in an imidazoquinoline. Bioorg Med Chem Lett. 2009; 19:2211–2214. [PubMed: 19285861]

41. Shukla NM, Mutz CA, Ukani R, Warshakoon HJ, Moore DS, David SA. Syntheses of fluorescent imidazoquinoline conjugates as probes of Toll-like receptor 7. Bioorg Med Chem Lett. 2010; 20:6384–6386. [PubMed: 20933417]

42. Shukla NM, Lewis TC, Day TP, Mutz CA, Ukani R, Hamilton CD, Balakrishna R, David SA. Toward self-adjuvanting subunit vaccines: model peptide and protein antigens incorporating covalently bound toll-like receptor-7 agonistic imidazoquinolines. Bioorg Med Chem Lett. 2011; 21:3232–3236. [PubMed: 21549593]

43. Baviskar AT, Madaan C, Preet R, Mohapatra P, Jain V, Agarwal A, Guchhait SK, Kundu CN, Banerjee UC, Bharatam PV. N-fused imidazoles as novel anticancer agents that inhibit catalytic activity of topoisomerase IIalpha and induce apoptosis in G1/S phase. J Med Chem. 2011; 54:5013–5030. [PubMed: 21644529]

44. Botos I, Segal DM, Davies DR. The structural biology of Toll-like receptors. Structure. 2011; 19:447–459. [PubMed: 21481769]

45. Jin MS, Kim SE, Heo JY, Lee ME, Kim HM, Paik SG, Lee H, Lee JO. Crystal structure of the TLR1-TLR2 heterodimer induced by binding of a triacylated lipopeptide. Cell. 2007; 130:1071–1082. [PubMed: 17889651]

46. Hemmi H, Kaisho T, Takeuchi O, Sato S, Sanjo H, Hoshino K, Horiuchi T, Tomizawa H, Takeda K, Akira S. Small anti-viral compounds activate immune cells via the TLR7 MyD88-dependent signaling pathway. Nat Immunol. 2002; 3:196–200. [PubMed: 11812998]

47. Weterings JJ, Khan S, van der Heden van Noort GJ, Melief CJ, Overkleeft HS, van der Burg SH, Ossendorp F, Van der Marel GA, Filippov DV. 2- Azidoalkoxy-7-hydro-8-oxoadenine derivatives as TLR7 agonists inducing dendritic cell maturation. Bioorg Med Chem Lett. 2009; 19:2249–2251. [PubMed: 19299126]

48. Kurimoto A, Hashimoto K, Nakamura T, Norimura K, Ogita H, Takaku H, Bonnert R, McInally T, Wada H, Isobe Y. Synthesis and biological evaluation of 8-oxoadenine derivatives as toll-like receptor 7 agonists introducing the antedrug concept. J Med Chem. 2010; 53:2964–2972. [PubMed: 20232824]

49. Hood JD, Warshakoon HJ, Kimbrell MR, Shukla NM, Malladi S, Wang X, David SA. Immunoprofiling toll-like receptor ligands: Comparison of immunostimulatory and proinflammatory profiles in ex vivo human blood models. Hum Vaccin. 2010; 6:1–14.

50. Warshakoon HJ, Hood JD, Kimbrell MR, Malladi S, Wu WY, Shukla NM, Agnihotri G, Sil D, David SA. Potential adjuvantic properties of innate immune stimuli. Hum Vaccin. 2009; 5:381–394. [PubMed: 19270494]

51. Kawai T, Akira S. TLR signaling. Semin Immunol. 2007; 19:24–32. [PubMed: 17275323]

52. Takeda K, Akira S. TLR signaling pathways. Semin Immunol. 2004; 16:3–9. [PubMed: 14751757]

53. Smirnov D, Schmidt JJ, Capecchi JT, Wightman PD. Vaccine adjuvant activity of 3M-052: An imidazoquinoline designed for local activity without systemic cytokine induction. Vaccine. 2011; 29:5434–5442. [PubMed: 21641953]

54. Ukani R, Lewis TC, Day TP, Wu W, Malladi SS, Warshakoon HJ, David SA. Potent adjuvantic activity of a CCR1-agonistic bis-quinoline. Bioorg Med Chem Lett. 2012; 22:293–295. [PubMed: 22104149]

55. David SA, Smith MS, Lopez G, Mukherjee S, Buch S, Narayan O. Selective transmission of R5-tropic HIV-1 from dendritic cells to resting CD4$^+$ T cells. AIDS Res Human Retrovir. 2001; 17:59–68. [PubMed: 11177384]

56. Kimbrell MR, Warshakoon H, Cromer JR, Malladi S, Hood JD, Balakrishna R, Scholdberg TA, David SA. Comparison of the immunostimulatory and proinflammatory activities of candidate Gram-positive endotoxins, lipoteichoic acid, peptidoglycan, and lipopeptides, in murine and human cells. Immunol Lett. 2008; 118:132–141. [PubMed: 18468694]
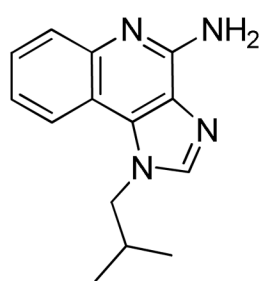
Imiquimod
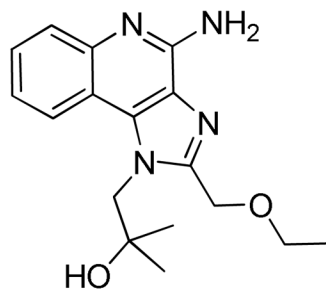
Resiquimod
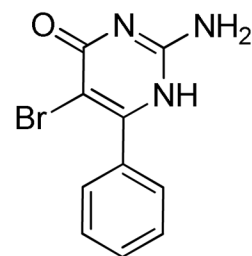
Bromopirone
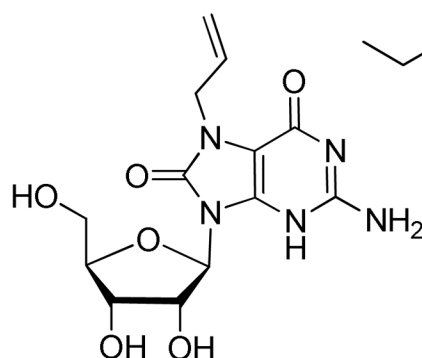
Loxoribine
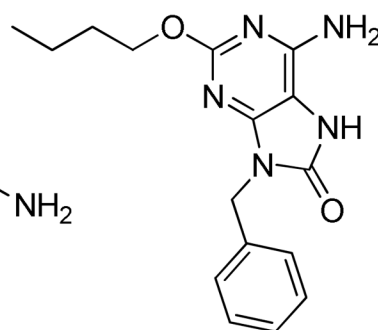
8-Oxoadenine derivative
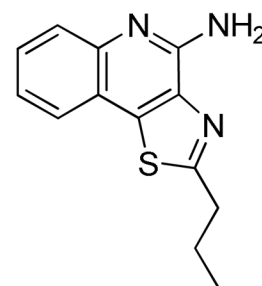
CL075

Figure 1.
Representative TLR7/8-agonistic heterocyclic small molecules.

1a: X = NR$_2$, **1b**: X = S,
1c: X = O, **1d**: X = Se

2

3

4
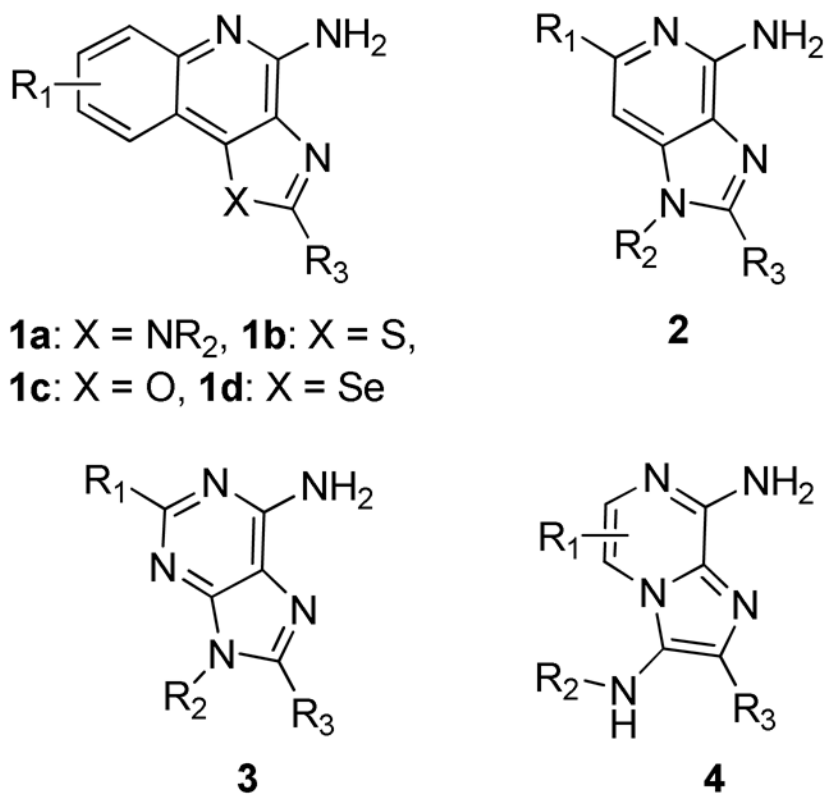
Figure 2.
TLR7/8 agonistic scaffolds. R$_1$ is typically alkyl or *O*-alkyl, R$_2$ is alkyl or benzyl, and R$_3$ is usually alkyl, and OH in oxoadenines.
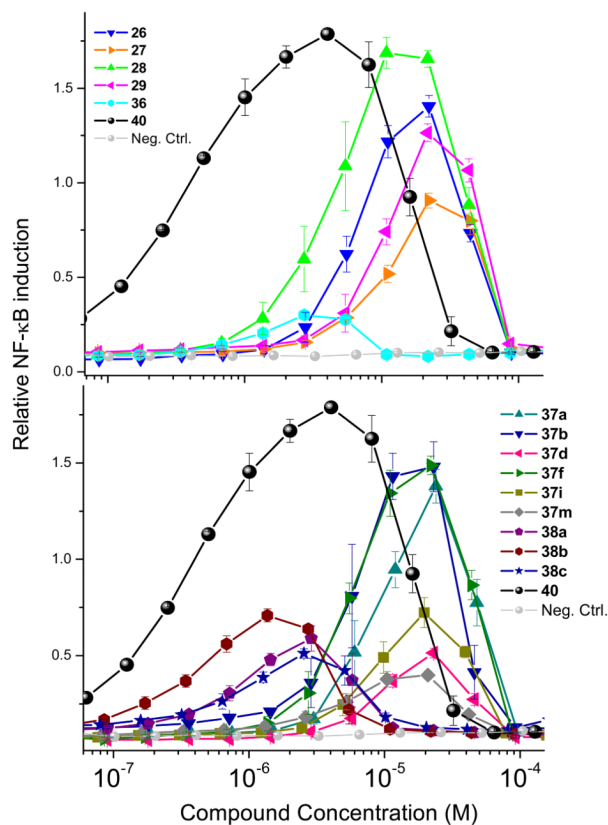
Figure 3.
Dose-response profiles of TLR8 agonism by select 2,3-diamino-furo[2,3-*c*]pyridines. Top: TLR8 agonism by compounds derived from Schemes 2 and 5. Bottom: TLR8 agonism by compounds derived from Schemes 6 and 7. Data points represent means and standard deviations obtained on quadruplicates.
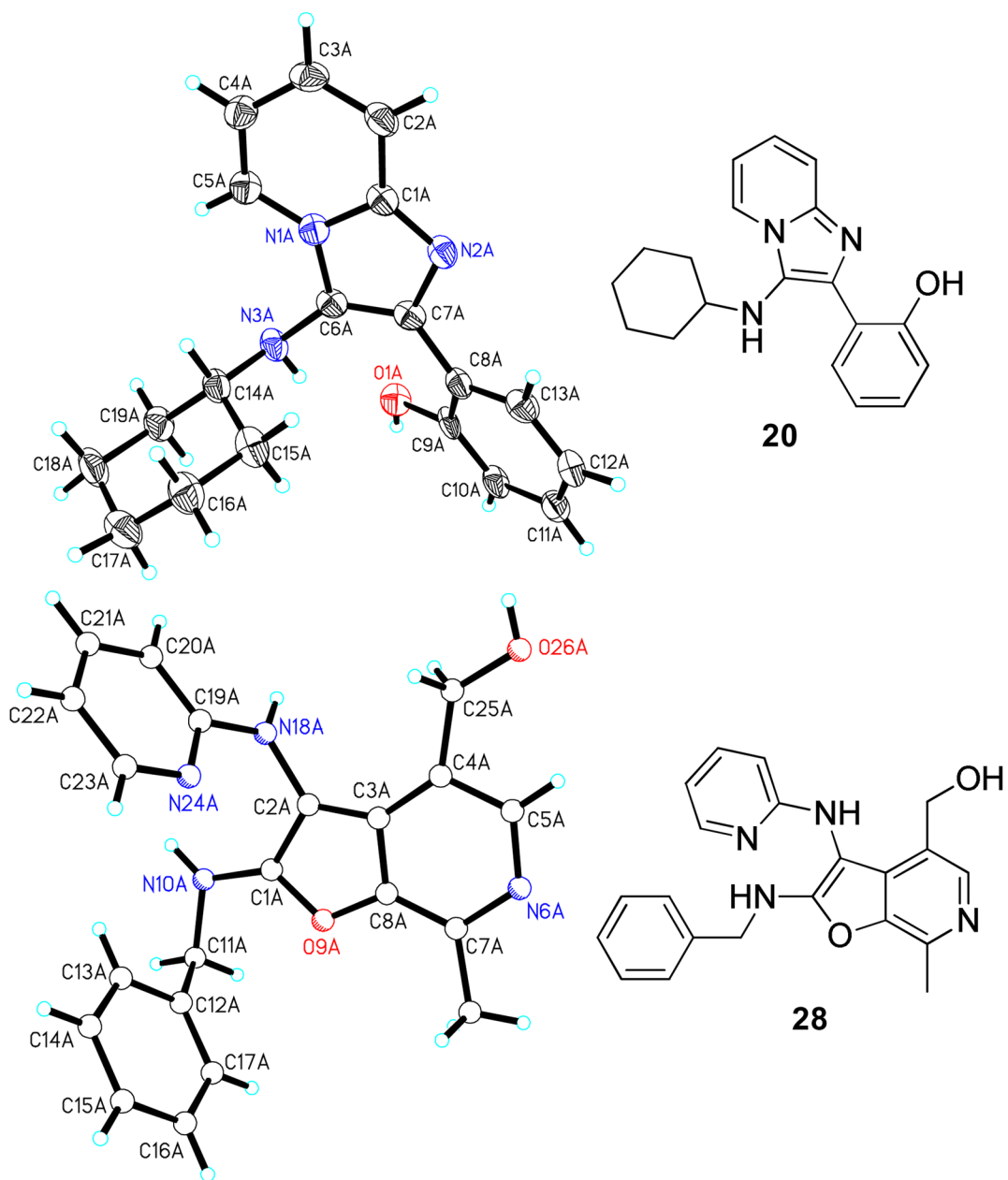
Figure 4.
Crystal structures of the salicylaldehyde-derived classic Groebke product (imidazo[1,2-
a]pyridine, **20**), and a non-Groebke, pyridoxal-derived furo[2,3-*c*]pyridine, **28**.
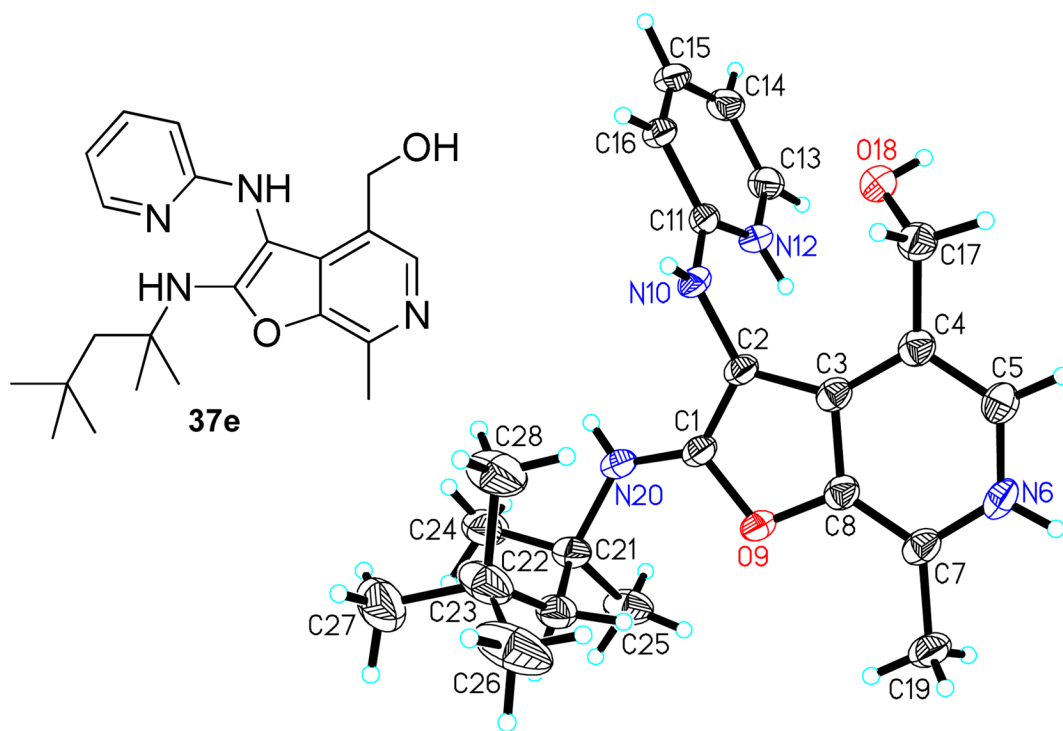
Figure 5.
Crystal structure (ORTEP view) of the non-Groebke furo[2,3-*c*]pyridine, **37e**, obtained with the use of pyridoxal as the aldehyde component.
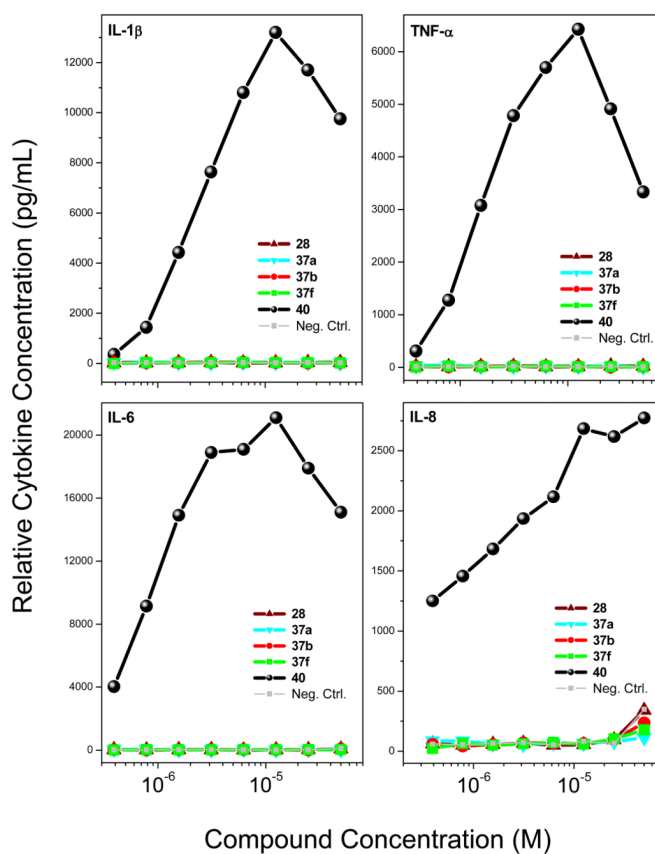
Figure 6.
Dose-response profiles of proinflammatory cytokine induction in hPBMCs by compounds
28, **37a**, **37b** and **37f**. Representative data from three independent experiments are
presented.
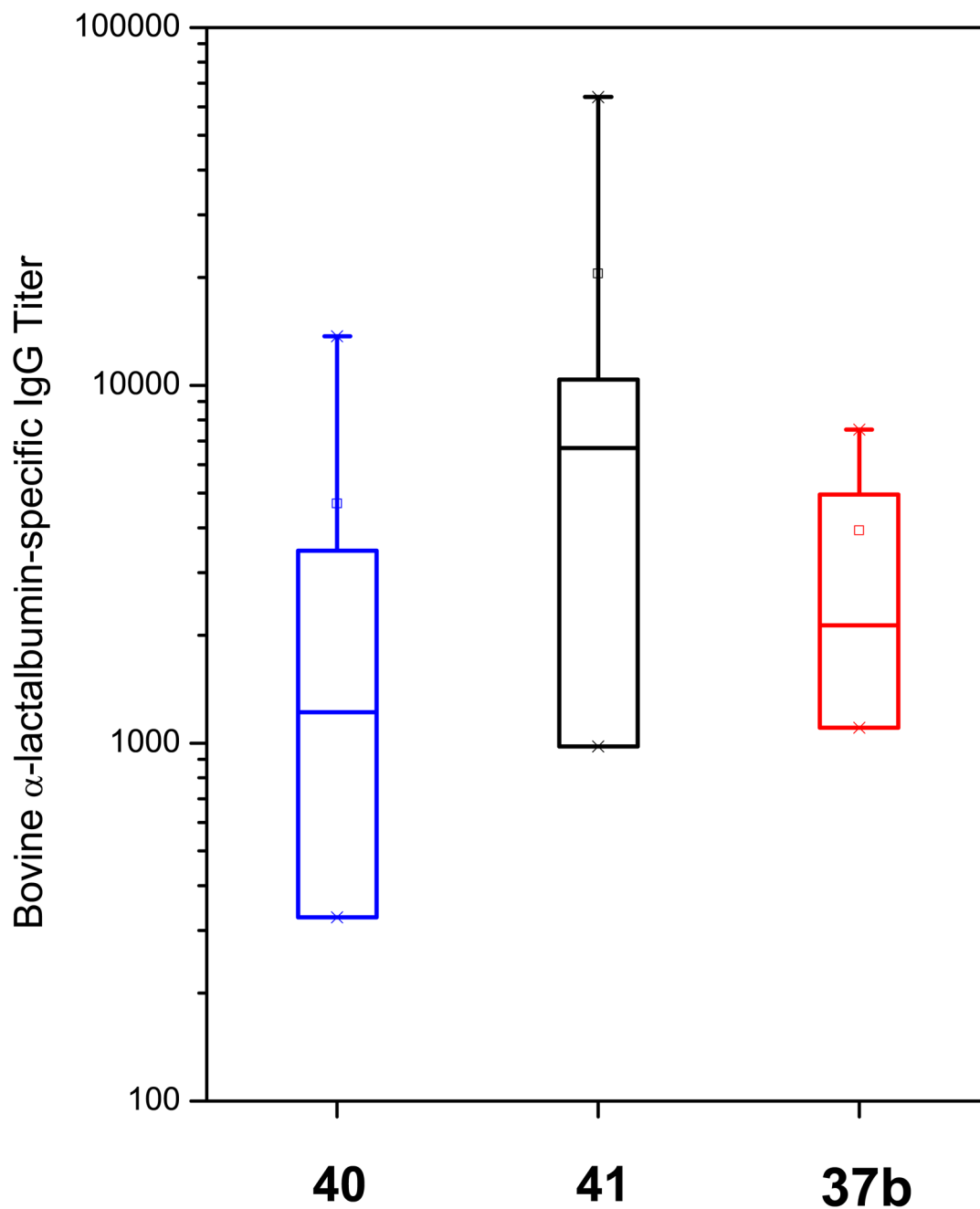
Figure 7.
Anti-bovine α-lactalbumin-specific IgG titers in rabbits adjuvanted with **37b**, **40**, and **41** (n=4, for each cohort). Box-plots of ratios of immune/pre-immune titers yielding absorbance values of 1.0 are shown for the individual samples. Means and medians of titers are represented by □ and – symbols within the box, respectively, and the X symbols indicate the 1% and 99% percentile values.
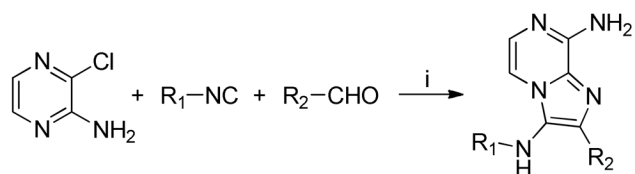
5a: R$_1$ = cyclohexyl, R$_2$ = Ph
5b: R$_1$ = cyclohexyl, R$_2$ = biphenyl
5c: R$_1$ = Bn, R$_2$ = C$_4$H$_9$
5d: R$_1$ = PhOMe, R$_2$ = C$_4$H$_9$

Reagents and conditions: i. (a) HCl in 1,4-dioxane, CH$_3$CN, MW 400W, 110 ^{o}C, 20 min; (b) Ammonium hydroxide, 110 ^{o}C, 16h

Scheme 1.
A two step one-pot synthetic process.
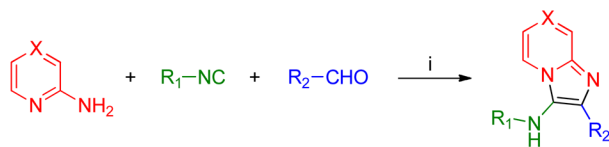
Reagents and conditions: i. HCl in 1,4-dioxane, CH$_3$CN, MW 400W, 110 °C, 20 min.
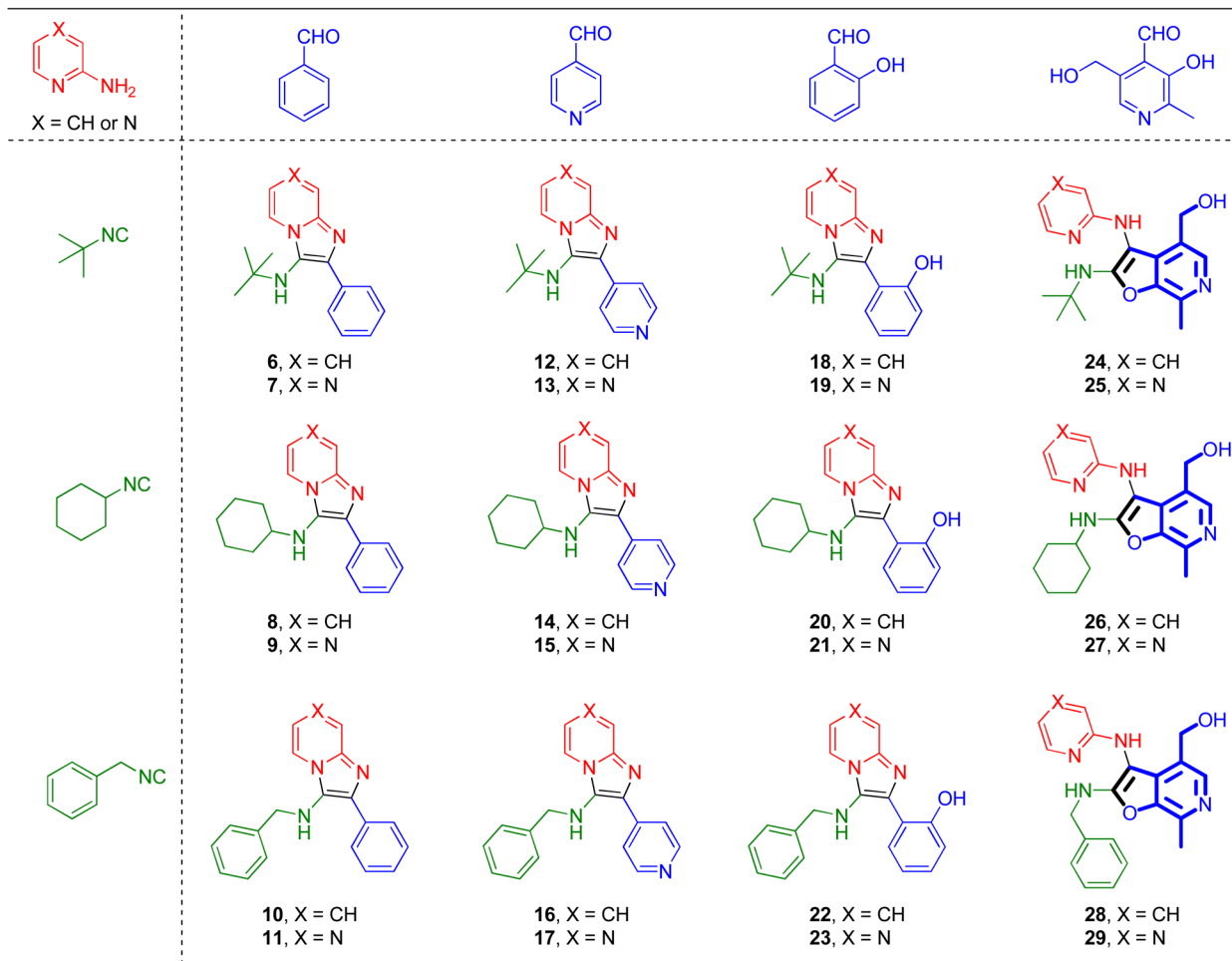
Scheme 2.
Twenty-four membered diverse test-library.
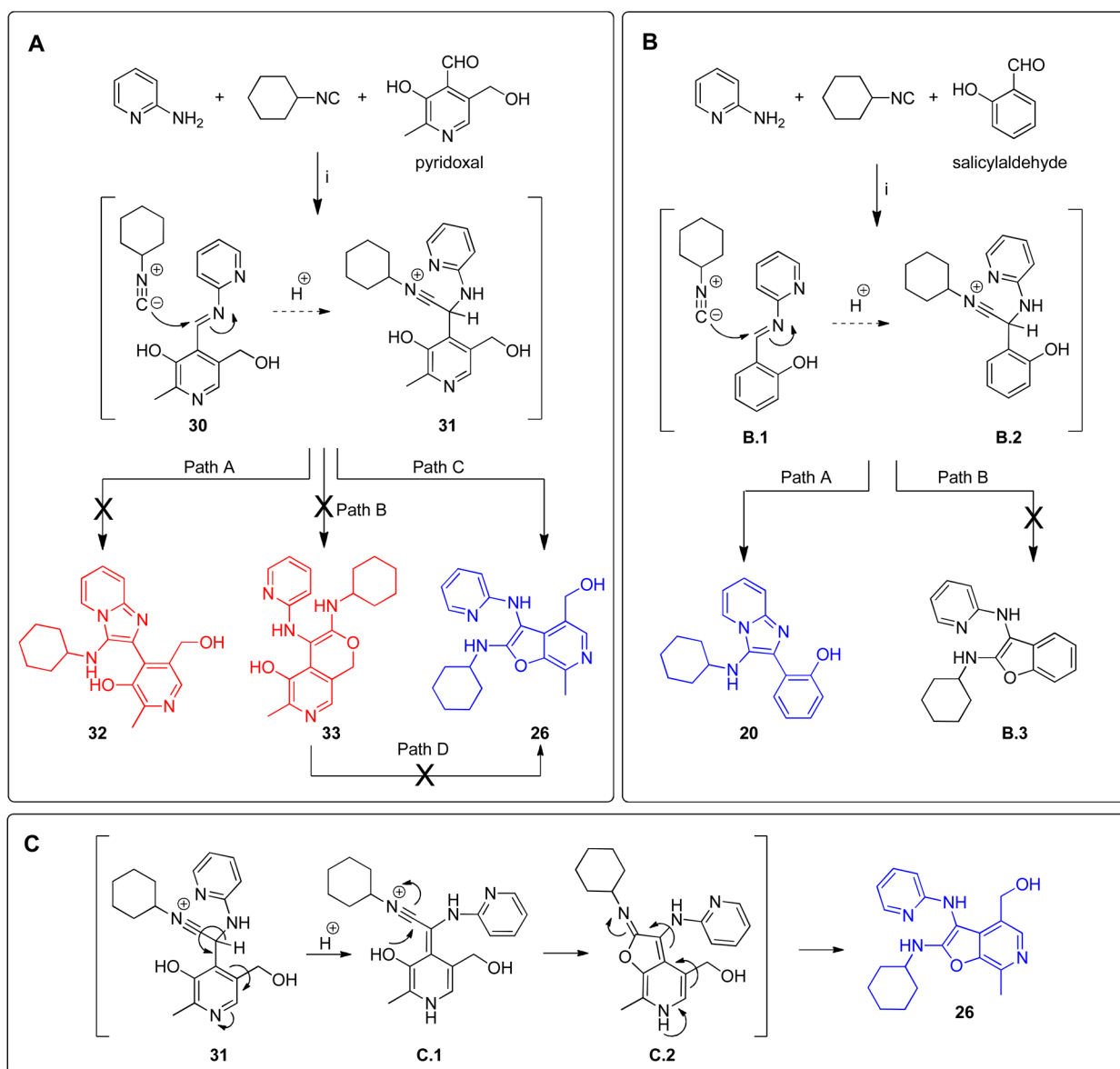
Reagents and conditions: i. HCl in 1,4-dioxane, CH$_3$CN or CH$_3$OH, MW 600W, 80 °C, 2 min.

Scheme 3.
Possible cyclization pathways and proposed mechanism.
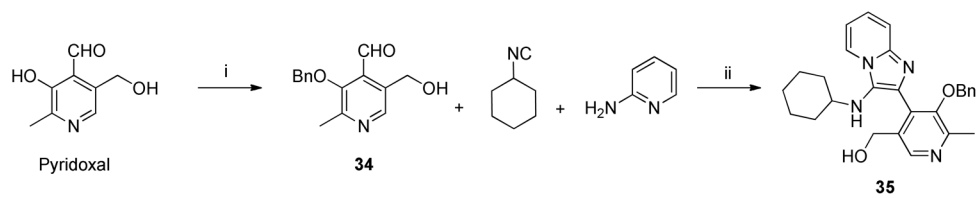
Reagents and conditions: i. BnBr, K$_2$CO$_3$, DMF, 25 ^{o}C, 16h; ii. HCl in 1,4-dioxane, CH$_3$CN, MW 400W, 110 ^{o}C, 20 min.
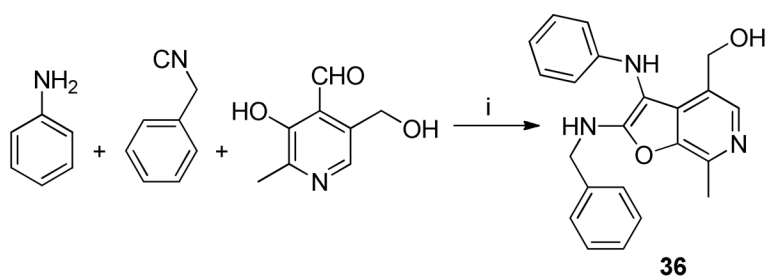
Scheme 4.

Reagents and conditions: i. HCl in 1,4-dioxane, CH$_3$OH, MW 600W, 80 $^{\circ}$C, 2 min.
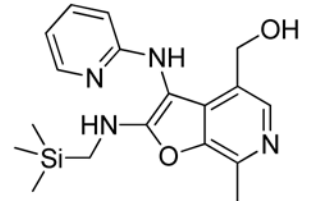
Scheme 5.
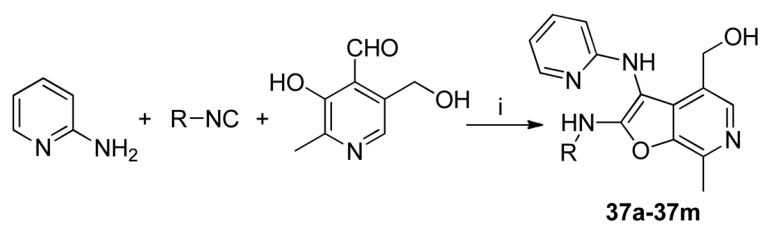
Various isonitriles used
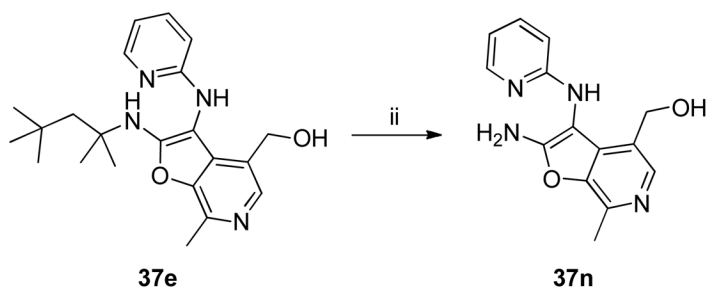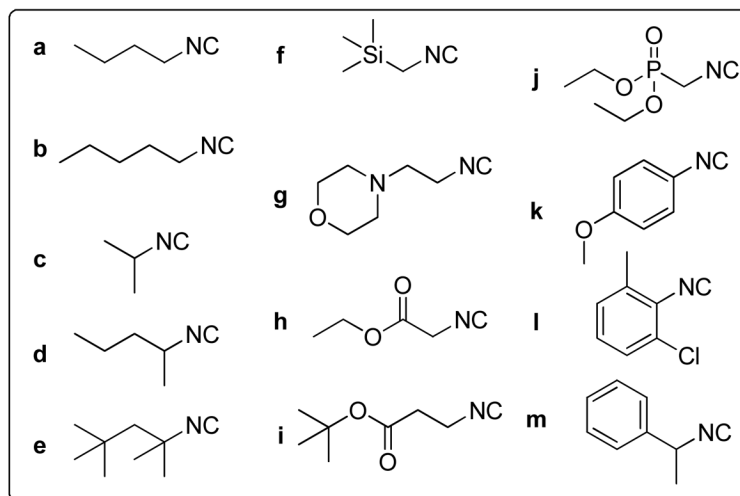
Reagents and conditions: i. HCl in 1,4-dioxane, CH₃CN, MW 600W, 80 °C, 2 min; ii. 50% TFA/CH₂Cl₂, 25 °C, 6h.
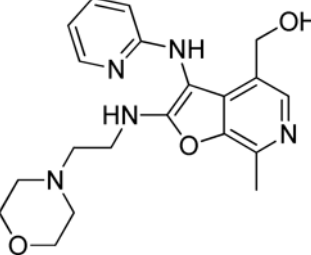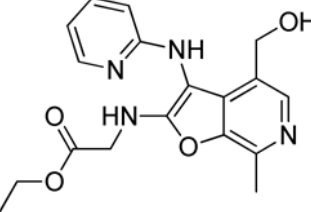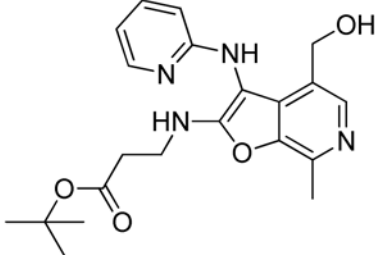
Scheme 6.
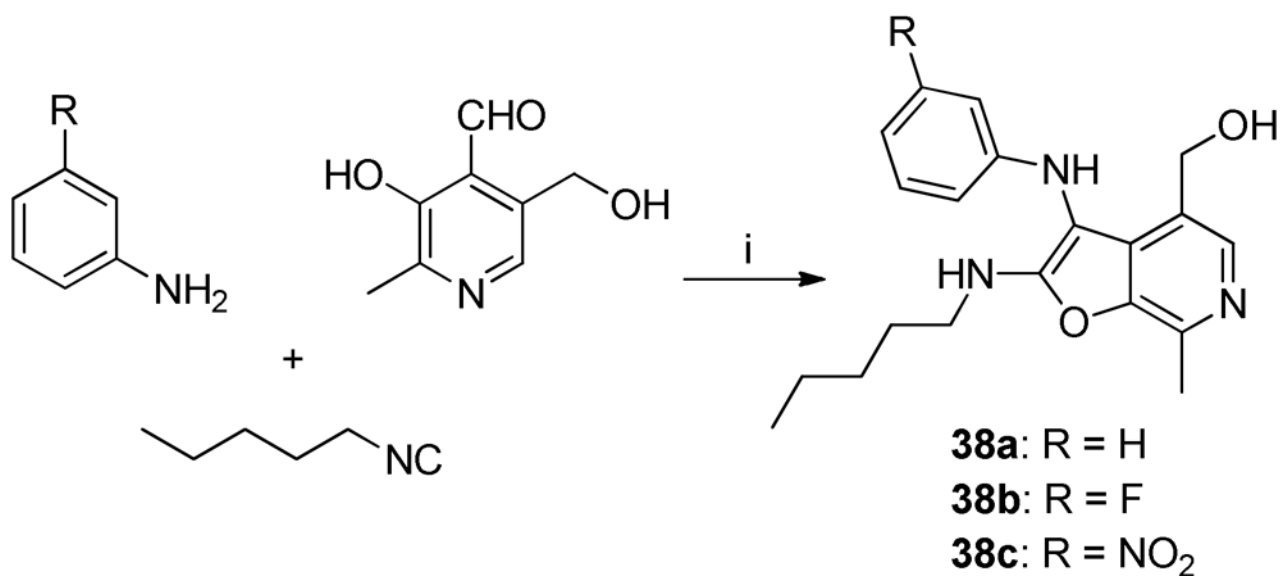
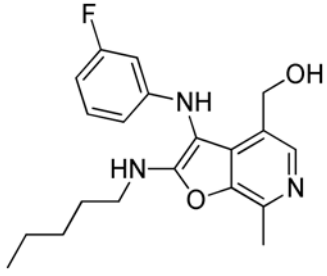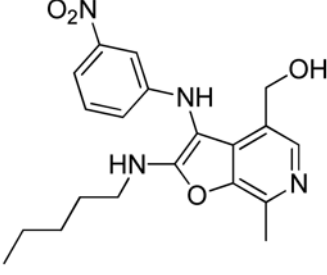Reagents and conditions: i. HCl in 1,4-dioxane, CH_3OH, MW 600W, 80 °C, 2 min.
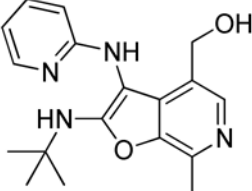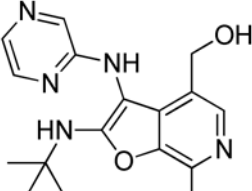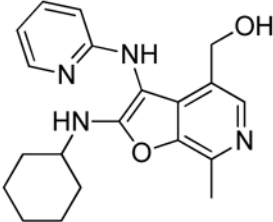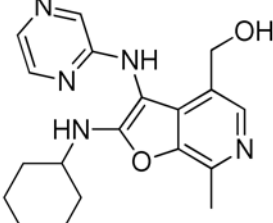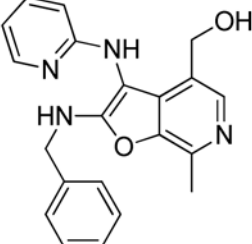
Scheme 7.
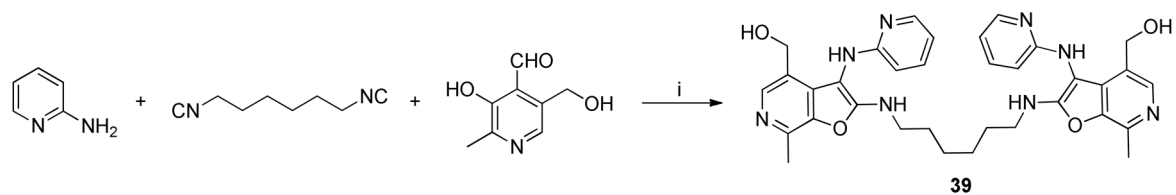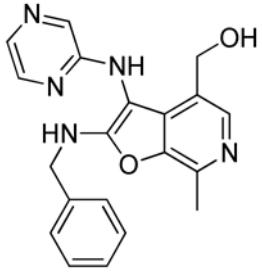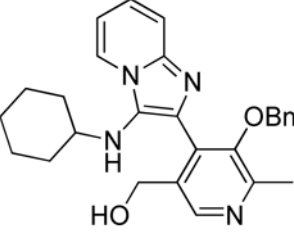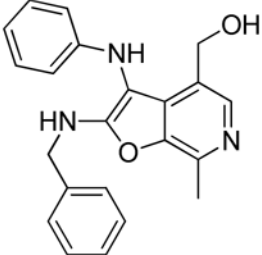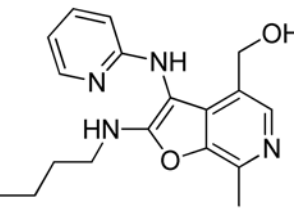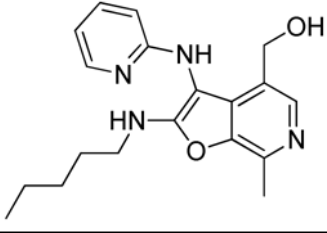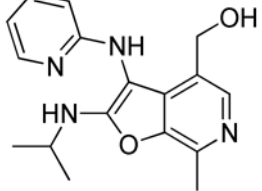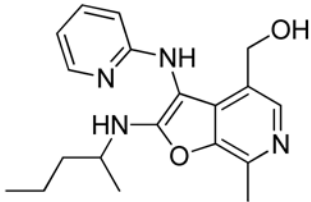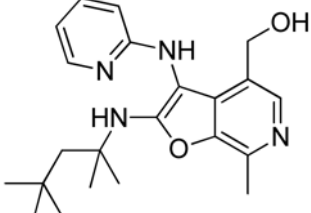
Reagents and conditions: i. HCl in 1,4-dioxane, CH$_3$CN, MW 600W, 80 °C, 2 min.
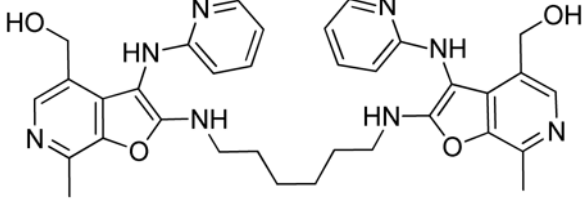
Scheme 8.

Table 1

EC$_{50}$ values of compounds in human TLR8-specific reporter gene assay

Structure	Compound Number	TLR8-Agonistic Activity (μM)
	24	Inactive
	25	Inactive
	26	6.93
	27	10.58
	28	4.91

Structure	Compound Number	TLR8-Agonistic Activity (μM)
	29	9.79
	35	Inactive
	36	1.68 Very low AUC
	37a	9.38
	37b	5.81
	37c	Inactive

Structure	Compound Number	TLR8-Agonistic Activity (μM)
	37d	9.01 Low AUC
	37e	Inactive
	37f	4.99
	37g	Inactive
	37h	Inactive
	37i	7.64 Low AUC

Structure	Compound Number	TLR8-Agonistic Activity (μM)
	37j	Inactive
	37k	Inactive
	37l	Inactive
	37m	4.27 Very low AUC
	37n	Inactive
	38a	2.25 Low AUC

Structure	Compound Number	TLR8-Agonistic Activity (μM)
	38b	0.37 Low AUC
	38c	0.85 Low AUC
	39	3.37